1.0

1.1

1.25   1.4

45
50

2.8   2.5

3.2   2.2

36

40   2.0

1.8

1.6

MICROCOPY RESOLUTION TEST CHART
NATIONAL BUREAU OF STANDARDS 1963-A

AFWAL-TR-80-4026

PILOT PLANT FORGING OF HYDROGENATED Ti-6Al-4V

W. R. Kerr

Structural Metals Branch
Metals and Ceramics Division

F. J. Gurney and I. A. Martorell
Westinghouse Electric Corporation

June 1980

TECHNICAL REPORT AFWAL-TR-80-4026

Final Report for Period February 1978 - June 1979

DTIC
ELECTE
SEP 2 3 1980

A

MATERIALS LABORATORY
AIR FORCE WRIGHT AERONAUTICAL LABORATORIES
AIR FORCE SYSTEMS COMMAND
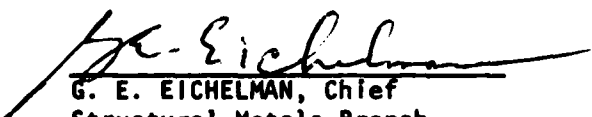WRIGHT-PATTERSON AIR FORCE BASE OH 45433

80 9 22 079

NOTICE

When Government drawings, specifications, or other data are used for any purpose other than in connection with a definitely related Government procurement operation, the United States Government thereby incurs no responsibility nor any obligation whatsoever; and the fact that the government may have formulated, furnished, or in any way supplied the said drawings, specifications, or other data, is not to be regarded by implication or otherwise as in any manner licensing the holder or any other person or corporation, or conveying any rights or permission to manufacture, use, or sell any patented invention that may in any way be related thereto.

This report has been reviewed by the Office of Public Affairs (ASD/PA) and is releasable to the National Technical Information Service (NTIS). At NTIS it will be available to the general public, including foreign nations.

This technical report has been reviewed and is approved for publication.

WILLIAM R. KERR
Project Monitor

FOR THE COMMANDER

G. E. EICHELMAN, Chief
Structural Metals Branch
Metals and Ceramics Division
Materials Laboratory
Air Force Wright Aeronautical Laboratories

REPORT DOCUMENTATION PAGE		READ INSTRUCTIONS BEFORE COMPLETING FORM
1. REPORT NUMBER AFWAL-TR-80-4026	2. GOVT ACCESSION NO. AD-A089 107	3. RECIPIENT'S CATALOG NUMBER
4. TITLE (and Subtitle) PILOT PLANT FORGING OF HYDROGENATED Ti-6Al-4V		5. TYPE OF REPORT & PERIOD COVERED Final Report. 30 February 1978—June 1979.
		6. PERFORMING ORG. REPORT NUMBER
7. AUTHOR(s) W. R. Kerr, F. J. Gurney and Dr. I. A. Martorell		8. CONTRACT OR GRANT NUMBER(s)
9. PERFORMING ORGANIZATION NAME AND ADDRESS Materials Laboratory Air Force Wright Aeronautical Laboratories (AFSC) Wright-Patterson Air Force Base OH 45433		10. PROGRAM ELEMENT, PROJECT, TASK AREA & WORK UNIT NUMBERS
11. CONTROLLING OFFICE NAME AND ADDRESS Same		12. REPORT DATE June 1980
		13. NUMBER OF PAGES 71
14. MONITORING AGENCY NAME & ADDRESS(if different from Controlling Office)		15. SECURITY CLASS. (of this report) Unclassified
		15a. DECLASSIFICATION DOWNGRADING SCHEDULE

16. DISTRIBUTION STATEMENT (of this Report)

Approved for public release; distribution unlimited.

17. DISTRIBUTION STATEMENT (of the abstract entered in Block 20, if different from Report)

18. SUPPLEMENTARY NOTES

19. KEY WORDS (Continue on reverse side if necessary and identify by block number)

Hydrogenation   Isothermal Forging
Ring Test   Titanium Alloy Ti-6Al-4V
Flow Stress

20. ABSTRACT (Continue on reverse side if necessary and identify by block number)

A pilot plant forging program for hydrogenated Ti-6Al-4V is described. The program was performed on ingot stock which was machined into ring shaped workpieces. The rings were hydrogenated to obtain hydrogen contents between 0.1 weight percent and 1.2 weight percent. A micro-balance technique was used to determine the hydrogen content. A description of the equipment and procedures for hydrogenation of the material and verification of the hydrogen analysis is given.

DD FORM 1473 EDITION OF 1 NOV 65 IS OBSOLETE
1 JAN 73

0.000126 m/s   0.0126 m/s

20. Abstract (Continued)

The ring forgings were performed on a hydraulic forge press using isothermal techniques. A temperature range between 922°K (1200°F) and 1144°K (1600°F) and deformation rates of 1.26x10^{-4}ms^{-1} (0.3 ipm) and 1.26x10^{-2}ms^{-1} (30.0 ipm) were used in the forging evaluation. Two heats of material were used. Three to six rings were forged at different reductions at each condition of temperature, rate and hydrogen content. Non-hydrogenated rings were also forged at each condition to form a baseline for comparison. Standard techniques were used to analyze the ring forging data.

Results from the program show that a 30 percent reduction in forging load results when material with approximately 0.4 weight percent hydrogen is used, utilized. At larger hydrogen contents, the deformation loads increase and are approximately equal to those for non-hydrogenated material when the hydrogen content is 0.8 weight percent. Deformation loads for the material with 0.4 weight percent hydrogen which are equivalent to those for non-hydrogenated produce occur at processing temperatures between 56°K (100°F) and 83°K (150°F) lower.

FOREWORD

This report was prepared by Mr. W. R. Kerr, Structural Metals Branch, Metals and Ceramics Division, Materials Laboratory, Air Force Wright Aeronautical Laboratories, Wright-Patterson Air Force Base, Ohio, and Mr. F. J. Gurney and Dr. I. A. Martorell of Westinghouse Electric Corporation, Advanced Energy Systems Division, Pittsburgh, PA. The work was performed under Work Unit 24180207, "Structural Metals."

The report covers work performed during the period 16 February 1978 to 30 June 1979.

Significant contributions to this report were made by Mr. T. E. Jones of Westinghouse who assisted in the design and operation of the hydrogenation system, and assisted in the forging studies and analysis of results. Thanks are also due to Mr. M. M. Myers and Mr. R. A. Sweeney of Westinghouse for their assistance in the forging studies, and to Mr. M. E. Rosenblum of Metcut, Materials Research Group for his assistance in dehydrogenation.

This technical report was submitted by the author February 1980.

Accession For

NTIS

Dist   Avail and/or
         special

TABLE OF CONTENTS

TABLE OF CONTENTS (Cont'd)

LIST OF ILLUSTRATIONS

LIST OF ILLUSTRATIONS (Cont'd)

LIST OF ILLUSTRATIONS (Cont'd)

LIST OF TABLES

SECTION I

INTRODUCTION

The absorption of hydrogen in titanium and titanium alloys has been a subject of concern for many years. From the phase diagram relationship (Reference 1), Figure 1, it can be seen that hydrogen stabilizes the high temperature bcc beta phase of titanium. The effect yields both deleterious and beneficial aspects.

The deleterious aspect of hydrogen in titanium is manifested by reduced notch ductility at room temperature. The residual effect of small amounts of hydrogen on reduced ductility can present a serious limitation to the utilization of these alloys in critical design applications (References 2, 3). A considerable amount of research on this effect has been accomplished which has established that hydrogen levels lower than 150 ppm would not result in a deleterious effect (Reference 3). Such levels can easily be obtained by simple vacuum annealing of the alloy.

While reduced room temperature ductility of hydrogen absorbed titanium poses a design limitation, it leads to a beneficial effect in the production of powder from these alloys (References 4, 5). At sufficiently high hydrogen contents a hydride phase, referred to as the gamma phase, develops what results in very brittle room temperature properties. The effect provides an economical means for the production of powder by simple crushing.

The enhanced stability that hydrogen imparts to the open structure beta phase, however, offers another potential benefit for high temperature forming. This effect is the inverse of that occurring in steels at the ferrite to austenite transformation where the higher temperature but close packed austenite requires higher forming loads than does the lower temperature but open structured ferrite. The inverse parallel effect in titanium can be even more beneficial since the amount of the less ductile hcp alpha phase is reduced or even eliminated at lower temperatures.

1

The enhanced processability effect of hydrogen on titanium is the subject of the research covered in this report. The investigation was performed on titanium alloy Ti-6Al-4V by forging hydrogenated ring specimens. Only forging results are covered in this report. Metallurgical interactions, unique microstructures, and service properties are to be covered in related reports.

SECTION II

BACKGROUND

1. DIRECT BENEFITS

Several investigations of effect of hydrogen on the processability of titanium alloys have been reported (References 6 through 9). These investigations have shown the direct benefits which may occur during high temperature forming of hydrogenated titanium alloys. These benefits include lower processing loads, improved processing ductility or workability, and lower processing temperatures (lower die temperature if isothermal).

The first effect, lower loads, is brought out graphically by results from investigations by Kolachev et al (Reference 8) for Ti-5Zr-9Al-5Sn-2Mo, Figure 2, and by Birla and DePierre (Reference 9) for Ti-6Al-2Sn-4Zr-6Mo, Figure 3. Very impressive reductions in upset forging pressures are also reported by Kolachev et al (Reference 7) for the alloy Ti-9Al. A non-hydrogenated ingot of the Ti-9Al alloy upset 1223K (950°C) to a deformation ratio of 25 percent, required a deformation pressure of 27 kg/mm^2, less than 25 percent of that for the non-hydrogenated product. (The hydrogen content was not specified). Results for the Ti-5Zr-9Al-5Sn-2Mo alloy (Reference 8) show a reduction in forging pressure of approximately 50 percent occurs when the alloy is hydrogenated to a level of 0.45 weight percent and forged at 1073K. However, the tensile strength for this alloy is reported (Reference 8) to drop from 30 kg/mm^2 for a hydrogen content of .003 weight percent to 3 kg/mm^2 for a hydrogen content of 0.45 weight percent, Figure 2. The results reported by Birla and DePierre (Reference 9) for the alpha-beta alloy, Ti-6Al-2Sn-4Zr-6Mo show a flow stress reduction of only 30-35 percent for the alloy containing approximately 0.4 weight percent hydrogen over that for non-hydrogenated product, Figure 3.

Improved workability of hydrogen containing titanium alloys has been well documented in the Russian work (References 7, 8). Upsetting of the Ti-9Al alloy (Reference 7) with 0.1 weight percent hydrogen at 1273K can be accomplished without cracking to 75-80 percent height reduction while

in the non-hydrogenated workpiece cracking occurred at greater than 35-40 percent height reduction. These results are explained by Kolachev et al (Reference 7) as attributable to two major effects. The first is that the introduction of hydrogen inhibits the precipitation of the grain boundary titanium aluminide, Ti_3Al (α_2), thereby promoting grain boundary sliding and yielding enhanced plasticity. A second effect is explained by Kolachev et al (Reference 7) by hydrogen promoting superplasticity through a reduction in the beta transus temperature and through a deduced argument that the presence of a high atomic percent content of hydrogen promotes enhanced diffusion of the titanium atoms.

It is possible that the evaluation technique itself may account for some of the results of Kolachev et al. The details of the processing conditions are not given, other than some of the forging was done using an air hammer. It is presumed that conventional temperature tooling was used with die temperatures between 573°K and 773°K. Processing alpha and alpha-beta titanium billets which are preheated just below the beta transus on conventional temperature tooling has been shown in other work (References 10, 11) to result in a significant amount of die chilling. This die chilling manifests itself by a loss in workability (Reference 10) and an increase in deformation pressure (References 10, 11). Both effects are owing to the die chilled portion of the workpiece transforming back to the low temperature alpha or alpha prime phase which is significantly less ductile than the beta phase and also significantly stronger. Hydrogenated alloys have considerably lower beta transus temperatures allowing a greater amount of chilling before the transformation would occur.

The third direct benefit of processing hydrogenated titanium alloys would result from the use of isothermal forging. The lower beta transus temperatures and enhanced workability would allow equivalent processability to be obtained at lower processing temperatures. The effects will allow lower cost die materials to be employed and also allow the selection of forging lubricants for this type of forging process to be simplified.

2. POTENTIAL BENEFITS

In addition to these direct benefits, other secondary benefits might be attained through associated processes. Of prime consideration is the production of titanium alloy powders by the hydride-dehydride process. The consolidation of already hydrided powders can yield the direct advantage just mentioned. Also, from the powder metallurgy viewpoint, a reduction in the contamination of the powder by oxygen would occur during handling and storage if the powder were kept in the hydride condition until after consolidation.

From the metallurgical viewpoint, improved deep hardenability, and unique metallurgical structures seem possible from controlled dehydrogenation. A parallel investigation of the optimization of microstructure through controlled time-temperature transformation of the hydrogen stabilized beta is underway at the Materials Laboratory (Reference 12).

It has been suggested (Reference 13) that during vacuum hot pressing of hydrogenated titanium alloy powder, the escaping hydrogen provides an ion scrubbing effect which removes contamination from the surface of the powder particles. The effect is a metallurgically cleaner product than would ordinarily be obtained from powder dehydrided prior to hot pressing or from powder produced by other techniques. The deformation of the powder under vacuum conditions can promote dehydrogenation through stress induced diffusion. The selective application of dehydrogenation during consolidation can be advantageous while interconnected porosity still exists. This would ensure short diffusion paths for the hydrogen and thus rapid dehydrogenation especially where thick components are considered. The process, however, also loses the advantage of low processing loads especially when the final stages of consolidation to theoretical density are attempted.

3. LIMITATIONS

Along with the known and possible advantages of processing
hydrogenated titanium alloys, certain limitations or disadvantages also
exist. The most obvious of these is that the material must be completely
dehydrogenated prior to use in a design application. This limitation
becomes aggravated whenever the thickness of the final product is large,
requiring long diffusion distances and consequently long diffusion times.

A second limitation to this process may occur with non-favorable
interactions among α-β phase changes, temperature and hydrogen diffusion.
As the hydrogen content is reduced during the dehydrogenation process,
the beta structure stabilizing effect is also reduced and a transformation
to the alpha structure occurs. Hydrogen diffusion through the hcp alpha
would be expected to be considerably slower than through the bcc beta
causing problems in removal of the lower concentration levels of hydrogen.

Residual stresses resulting from volumetric changes during dehydro-
genation of certain geometric shapes may also cause difficulties. In
the case of a thin inner disk with a more massive outer hub, it would be
expected that dehydrogenation would occur quickly in the thin disk and
more slowly in the thick hub. Shrinkage stress and possibly plastic
deformation would result.

A final potential problem that must be investigated is the possibility
of void development during dehydrogenation. This would be especially
critical when non-uniform geometries are dehydrogenated and when second
phase particles with limited solubility for hydrogen are incorporated
into the titanium alloys.

While all of the direct and potential benefits as well as the
limitations of the process must be considered to determine technical
and economic feasibility, this complete spectrum of the problem will not
be covered in this report. Rather the effort of this report is directed
solely at the processing portion of the total effort.

SECTION III

EXPERIMENTAL PROGRAM

1. MATERIAL

The material selected for the initial phase of the investigation was titanium alloy Ti-6Al-4V. The reason for selection of this alloy was primarily because of its wide acceptance in the industry and because it forms a baseline for many alloy development and research programs.

In the preceding section it was argued that it would be economically more advantageous to work with already hydrogenated powder produced by the hydride-dehydride process. However, quality control problems presently exist with this powder process and therefore it was decided instead to perform the initial evaluation on commercial ingot stock which would be subsequently hydrogenated.

The material was procured in the form of two-inch diameter bars. Two bars, each from different heats were purchased. The chemical analyses of each heat are given in Table 1. Approximately 100 ring specimens were machined from each bar for forging flow stress evaluation. The ring dimensions were 1.980 in. O. D., 0.990 in. I. D. and 0.330 in. thick.

2. HYDROGENATION PROCEDURES

   a. Theoretical Basis

      Initial estimates for the time-temperature conditions for diffusion of hydrogen were based on data from the literature (References 14 through 16). From this preliminary analysis it was estimated that hydrogenation could be accomplished at reasonable rates through the thickness of the ring specimen in the temperature regime of 867°K (1100°F) to 1144°K (1600°F). The data (References 14 through 16) also show that the amount of hydrogen which will be absorbed is related to the partial pressure of the supply gas. This information provided the basis for setting up the equipment for hydrogenation.

b. Hydrogenation Equipment

Hydrogenation was accomplished in the apparatus shown schematically
in Figure 4. The hydrogenation chamber consists of a Type 304 stainless
steel tube 3 in. O. D. x 0.63 in. wall. Flanges of the same material
were welded to both ends and closure achieved by means of O-ring seals
and bolted port cover. The cover at one end had penetration for inlet
and outlet tubes and for the recording thermocouples. The hydrogenation
tube was approximately 5 inches long and was centered in a 30 inch long
Dynatherm tube furnace. A uniform temperature work zone ten inches long
was achieved. Temperature was controlled by a chromel alumel thermo-
couple placed between the tube and the furnace wall using a Lindberg SCR
Controller. Temperature was recorded within the work zone by three
sheathed chromel-alumel thermocouples and a Honeywell twelve point
recorder. Temperature within the work zone was uniform within $\pm$ 10°K.

Stainless steel tubes, 1/4 in. O. D. x .010 in. wall were used for
the inlet and outlet of the gas. Holes were drilled at one inch intervals
along the length of the inlet tube within the work zone. To improve
uniformity of flow and hydrogen distribution within the work zone, the
diameter of these holes varied, being smaller nearer the inlet end where
the inlet pressure was greater. A single hole was drilled in the outlet
tube at the center of the work zone. With this configuration and a total
gas flow of approximately 2 1/4 liters/minute through the furnace, the
absorption of hydrogen by samples within the work zone was found to be
symmetrical about the center although not necessarily uniform. Gas was
supplied from standard cylinders. Argon plus 4 percent hydrogen was
purchased premixed. This mixture is non-flammable and may be treated as
an inert gas yet it has a hydrogen partial pressure high enough to be
in equilibrium with an appreciable hydrogen concentration in titanium
(~1 weight percent in pure titanium). The relative proportion of
hydrogen and argon in the hydrogenating mixture was controlled by
adjusting the individual flow meters on the argon 4 percent hydrogen,
on the hydrogen, and on the argon bottles. Flow through the system
and leakage were monitored by means of the inlet and outlet flow meters.

The outlet was provided with a bubbler containing diffusion pump oil to prevent back diffusion of air into the system. A dry bottle was included to prevent pulling the oil from the bubbler out into the furnace in the event the valves were not completely closed. Outlet gas containing hydrogen was burned by passing the gas through a natural gas flame. The entire apparatus (except for gas bottles) was enclosed in a fume hood.

Rings to be hydrogenated were placed in an appropriate rack and loaded into the work zone through the loading port. The port was sealed, and the system was evacuated by means of a mechanical pump and purged with argon three times. A flow of argon of approximately 1/2 liters/ minute was maintained while the furnace tube was heated to temperature. The hydrogen was added to the argon flow after the rings reached the hydrogenating temperature. All rings were hydrogenated at 650°C (1200°F). The relative proportions of hydrogen and the time required for the hydrogenation were determined empirically depending upon the number and size of specimen and the hydrogen content required. The hydrogen partial pressures ranged between .5 atm and .95 atm; times varied between 1/2 hour and 2 hours. The flow of inert gas was maintained with the hydrogen flow as a safety measure to prevent back of flow of air into the furnace and to eliminate the danger of explosive air-hydrogen mixture.

At the end of the pre-determined hydrogenation time, the flow of argon and hydrogen were replaced by a flow of argon -4 percent hydrogen. The outlet valve was then closed and the system pressurized to ~2 psi by means of the gas regulator. The rings were allowed to soak at temperature in this gas mixture to permit diffusion within the rings to achieve a uniform hydrogen content. At the end of the soak time, the furnace was shut-off and allowed to cool to room temperature.

The limited volume of the work zone relative to the rings did not allow sufficient control of the hydrogen flow and distribution to ensure uniform absorption by the rings. Rings at the ends of the work zone absorbed more hydrogen than those in the center. To compensate for this effect, rings were hydrogenated at least two times with their positions reversed (center to ends, ends to center) between cycles.

c. Hydrogen Analysis

Determination of the hydrogen content of the various specimens used in the Hydrovac program presented something of a problem. Conventionally, the hydrogen content of titanium is determined by melting the sample or heating it to high temperature, collecting and measuring the gas released assuming (validly) that only hydrogen will be removed from titanium alloys. The difficulty with this technique is that the system used is designed for relatively low hydrogen concentrations (of the order of a few hundred ppm). The large concentration used in this program tended to overwhelm such a system, unless very small sample sizes were used. This latter alternative presented a sampling problem. Further, submitting each specimen for hydrogen analysis would be very expensive in terms of analytical costs.

The hydrogen concentrations reported in this program are based on weight changes. Specimens were weighted on an analytical balance capable of measuring 0.1 mg with a reproducibility of $\pm$ 0.2 mg. For a 50 gram ring specimen containing 0.1 percent hydrogen, the balance was capable of a theoretical accuracy of $\pm$ 4 percent of the hydrogen present. Theoretically, the accuracy would be better for higher hydrogen concentrations. Actual accuracy was somewhat less. The tendency of titanium to absorb oxygen and other interstitials even in relatively inert atmospheres and the vapor pressure of titanium at higher temperatures in vacuum, tended to complicate the analysis problem. Table 1 shows a comparison of hydrogen contents based on weight gain with contents obtained by vacuum fusion analysis. With one exception, the concentrations vary within 10 percent or less. The vacuum fusion analysis tends to give higher hydrogen contents than indicated by weight gain. In view of the fact that the weight gain concentration was based on a relatively large sample and the vacuum fusion sample was cut using a lubricant which may have added hydrogen, it is difficult to suggest that the vacuum fusion analysis was indeed more accurate.

As a check on the weight gain as a measure of hydrogen content, a number of specimens were weighed, hydrogenated, reweighed, dehydrogenated

in a vacuum furnace, weighed again, and finally sections were submitted
for vacuum fusion analysis. Results were shown in Table 2. Hydrogen
contents based on weight gain and weight loss agree within 3 percent.
Hydrogen contents based on weight loss appear to be consistently lower
than those based on weight gain. Table 3 shows the weight loss and
gain of specimen run through the hydrogenation cycle and dehydrogenation
cycle with no hydrogen added. The weight gains of these specimens
during the dehydrogenation cycle may be attributed to oxygen pick up.
If this average gain is used to correct the weight losses in Table 2,
the hydrogen contents agree $\pm$ 1 percent.

d. Post-Hydrogenation Diffusion Barriers

It was necessary to determine the amount of hydrogen lost from the
samples during normal post-hydrogenation handling, including preheating
prior to forging. For this purpose, 2 inch diameter disks were hydrogenated
to approximately 0.9 weight percent hydrogen. Some specimens were left
uncoated, some were coated with glass frit (Delta Glaze 149) and air
dried. The glass coating of some of the samples was fused by heating
in an argon -4 percent hydrogen atmosphere at 977°K (1300°F). Assuming
that hydrogen loss would be diffusion controlled and therefore inversely
proportional to thickness, three specimen thicknesses were used, 1/8 inch,
1/4 inch and 1/2 inch. The specimens were then heated in air to forging
temperatures for various times.

After exposure in the air furnace, the specimens were grit blasted
to remove the coating or the oxide which resulted on the uncoated
specimens. A one inch square was cut from the center of each disk to
eliminate possible hydrogen pickup from the cutting lubricant. The
specimens were cleaned ultrasonically in acetone and methanol and weighed.
They were dehydrogenated at 1273°K (1800°F) in a vacuum furnace which
attained a final vacuum pressure of approximately 5×10^{-6} torr. The
specimens were then weighed and the hydrogen content determined.

Results of these experiments are shown in Table 4. It is apparent
from the data that no pattern exists with respect to disk thickness.

AFWAL-TR-80-4026

No significant difference in hydrogen retention resulted from variations
in time at temperature. It would appear therefore, that hydrogen
retention is not diffusion controlled. The naturally occurring oxide
film on the specimen was sufficient to prevent hydrogen loss. More
consistent results were obtained with specimens coated with the glass
frit, and since the glass is required as a lubricant, this coating was
used for the forging studies. The results obtained with fused glass
specimen were slightly better than for those coated with the glass frit
but the difference did not justify the additional effort involved in
producing the fused coating.

3. FORGING TESTS

   a. Forging Equipment

The forging equipment used for this program was the 4.4×10^4N (500 Ton)
Hydraulic Forge Press located at the Materials Laboratory. A slow-speed
ram motion system has been adapted to the press. The slow-speed system
entails an auxiliary hydraulic system which is activated through high
pressure valves after the main hydraulic system of the press has been
isolated. Controlled speed ram motion is achieved through a closed
loop electrical control system to achieve ram speeds between 1.26×10^{-5}ms^{-1}
(0.030 ipm) and 2.1×10^{-3}ms^{-1} (5.0 ipm). The conventional or standard
ram motion control system allows the achievement of speeds up to
1.26×10^{-1}ms^{-1} (300 ipm). Ram speeds of 1.26×10^{-2}ms^{-1} (30 ipm) and
1.26×10^{-4}ms^{-1} (.3 ipm) were used in this investigation.

Forging dies heated to the same temperature as the specimen were
used in this study. The forging dies were heated with high temperature
cartridge heaters inserted into an M-246 nickel base superalloy die block
with 713C alloy flat dies positioned on the heated die block. The entire
die system was enclosed in a chamber to prevent air flow over the dies.
Supplemental heat for the die chamber was supplied from Kanthal
resistance coil heaters imbedded in ceramic plates which were located
on two opposing interior surfaces of the die enclosure chamber. These
plates were positioned as near as possible to the movable die system

12

to ensure temperature uniformity over the surface of the dies. Temperature control for each region of supplied heat was achieved through use of SCR type controllers. Die temperatures between 922°K (1200°F) and 1144°K (1600°F) were used in this program.

b. Forging Testing Procedures

The ring compression test was used in this program to determine flow stress variations introduced by different levels of hydrogenation, forging temperatures, and forging rates. Non-hydrogenated and dehydrogenated rings were also forged to obtain comparison effects. Details of this test procedure with appropriate references are given in the Appendix.

Prior to forging, each ring specimen was cleaned in acetone and coated with a commercially available glass base coating. The coating utilized was Delta Glaze 149 manufactured by Acheson Colloids. After coating, the ring was preheated for 30 minutes in an air atmosphere electrical resistance furnace at the desired forging temperature. The specimens were transferred manually with tongs onto the forging dies which were heated to the same temperature as the workpiece preheating furnace. Five rings each with the same level of hydrogen were forged to different reductions at each temperature. The nominal height reductions were 15, 30, 40, 40, 50, and 60 percent. After forging, the rings were cleaned, measured and evaluated as outlined in the Appendix.

SECTION IV

RESULTS

1. HYDROGEN CONTENT AND FORGING TEMPERATURE VARIATIONS

The deformation loads and geometry changes in ring dimensions are used to calculate flow stress using the ring compression test outlined in the Appendix. The stress strain relations thus obtained for the first heat of material with nominal hydrogen levels of 0, .4, .8 and 1.2 weight percent and forged with a ram velocity of $1.26 \times 10^{-4} \text{ms}^{-1}$ (0.3 ipm) at temperatures of 922°K (1200°F), 1033°K (1400°F), 1089°K (1500°F) and 1144°K (1600°F) are plotted in Figures 6 through 9. With the exception that the flow stress drops with increasing temperature, the relations are all quite similar. The lowest level of flow stress results from the workpieces with 0.4 weight percent hydrogen and the highest level of flow stress results from the workpieces with 1.2 weight percent hydrogen. The flow stresses for workpieces with 0.8 weight percent hydrogen are initially higher than that for workpieces without hydrogen, but at strain levels of about 0.2 to 0.3 in./in. the flow stress becomes less than that for the non-hydrogenated condition for all temperatures investigated except at 1089°K (1500°F).

2. FORGING RATE VARIATIONS

When the forging rate is increased by a factor of 100, the flow stress of the material increases as expected. This effect is illustrated in Figures 10 and 11 for material from the first heat hydrogenated to levels of 0.4, 0.8 and 1.2 weight percent and forged at 1033°K (1400°F) and 1144°K (1600°F). With slight variations, the effect of hydrogen content is nearly the same as found for lower deformation rates.

3. HEAT-TO-HEAT VARIATIONS

Initial investigations on the second heat of material concentrated on lower levels of absorbed hydrogen, between .1 and .575 weight percent. Stress strain results for these hydrogen contents forged at $1.26 \times 10^{-4} \text{ms}^{-1}$ (0.3 ipm) are presented in Figures 12 and 13 for temperatures of

922°K (1200°F) and 1033°K (1400°F) respectively. The configuration of
the stress-strain curves for this heat of material is slightly different
than for those from the first heat, but again show that the lowest flow
stress is obtained at approximately 0.4 weight percent hydrogen,
Figure 13.

Results from forging of the second heat of material at the higher
rates $1.26 \times 10^{-2} ms^{-1}$ (30 ipm) are shown in Figures 14 and 15 for 1033°K
(1400°F) and 1089°K (1500°F) forging temperatures respectively. Again
the same general configuration of stress strain relation is noted. A
distinct shift to lower hydrogen contents is noticeable in the minimum
flow stress. A hydrogen level of 0.3 weight percent yields the lowest
flow stress for the 1033°K (1400°F) forging condition, Figure 15. When
the forging temperature is raised to 1144°K (1600°F) the alloy with only
0.2 weight percent hydrogen content yields slightly lower stress levels.
Microstructural examination of material after forging at 1144°K (1600°F)
indicates that the structure becomes completely beta between hydrogen
contents of 0.2 and 0.3 weight percent, Figure 16.

4. TRANSFORMATION INDUCED VARIATIONS

Further investigations conducted on the second heat of material to
determine the effect of the transformation itself are presented in
Figures 17 through 22. The basic variation examined entailed hydro-
genation of the workpieces at 922°K (1200°F) to hydrogen levels of
.4, .8 and 1.2 weight percent. These hydrogenated rings were then
exposed to an all beta temperature condition 1144°K (1600°F) for 1/2
hour and directly transferred to an aging furnace at 867°K (1100°F)
and held for 4 hours. After aging, one-half of the rings were vacuum
dehydrogenated by the standard technique. The ring specimens were then
glass coated, heated to the desired temperature and then isothermally
forged at $1.26 \times 10^{-4} ms^{-1}$ (0.3 ipm). Results for workpieces hydrogenated
to a level of .4 and 1.2 weight percent and then forged at 922°K (1200°F)
are presented in Figures 17 and 18 respectively. The results follow
closely those presented in Figure 6 where hydrogen levels of .4 weight
percent reduce the flow stress and those levels of 1.2 weight percent
hydrogen increase the flow stress.

With some variations at strains greater than 0.5, the flow stress for
the dehydrogenated conditions are approximately the same for material
initially hydrogenated to a level of 0.4 or 1.2 weight percent. When
these dehydrogenated conditions are compared to material from the same
heat which had never been hydrogenated nor exposed to an all beta
condition but otherwise forged in the same manner, Figure 12, some
additional variations in the flow stress were noticeable, especially at
the low strain levels where starting microstructure would be expected
to play the greatest effect.

Flow stress results from rings forged at 1033°K (1400°F) instead of
922°K (1200°F) but at otherwise identical conditions show similar effects.
These effects are illustrated in Figures 18 and 19.

A more extensive variation of the transformation effects of hydrogen
was investigated with workpieces hydrogenated to the 0.8 weight percent
level. Two transformation variations and two dehydrogenation variations
were introduced. The first transformation condition was the same as that
utilized for the 0.4 and 1.2 weight percent conditions, heating to
1144°K (1600°F) for 1/2 hour and then transferring directly to a second
electric resistance air atmosphere furnace at 867°K (1100°F) and holding
for an additional 4 hour period and then air cooling. The second
transformation variation also began with heating to 1144°K (1600°F) for
1/2 hour, but the specimens were then allowed to air cool to room
temperature. After cooling, the specimens were then placed in an electric
resistance air atmosphere furnace preheated at 867°K (1100°F) and held
there for a period of 2 hours. The two dehydrogenation conditions
differed in the temperature used. The first dehydrogenation was conducted
at 922°K (1200°F) and the second at 1033°K (1400°F). In both cases the
dehydrogenation time used was that required to achieve a pressure of
$10^{-6}\mu$.

The results of these variations are shown in Figures 21 and 22.
These results show somewhat higher deformation pressures than resulted
from Heat A (Figure 6) but show the same general trends. The material

containing hydrogen has an initially lower flow stress than that
material without, but at a strain of approximately 0.3 in./in. this effect
is reversed and the hydrogenated material then requires the higher
deformation loads. While some effect of the different dehydrogenation
and different transformation effects did occur, these effects did not
show strong trends.

SECTION V

DISCUSSION

1.   EFFECTS OF HYDROGEN CONTENT ON THE FLOW STRESS OF Ti-6Al-4V-H

When the flow stress data from Figures 6 through 9 are considered
in terms of the hydrogen content, it can be seen that a minimum in the flow
stress occurs at a hydrogen content of approximately 0.4 weight percent,
Figure 23. Hydrogen contents greater than this amount cause an increase
in the flow stress where hydrogen content of approximately 0.8 weight
percent yield approximately the same flow stress as non-hydrogenated
material.

The decrease in flow stress with increasing hydrogen content is
expected when consideration is given to hydrogen stabilizing the open
bcc beta structure of titanium. This portion of the results are similar
to those already reported in the literature (References 5 through 9).
However the increase in flow stress for alloys with hydrogen contents
greater than 0.4 has not been previously reported and shows a type of
alloy strengthening effect. Other investigations on this effect
(Reference 12) indicate that the gamma phase, TiH, is appearing in the
structure and causing the strength increase. The phase relationships
for Ti-6Al-4V and hydrogen appear to be significantly different
(Reference 12) from those shown in Figure 1 for the titanium-hydrogen
binary.

It should be pointed out that the data of Kolachev et al (References
7, 8) do not include hydrogen concentrations greater than 0.45 weight
percent. Since the base alloys investigated by Kolachev et al (References
7, 8) are of high aluminum content it is possible that the gamma phase
would not be experienced until significantly higher hydrogen levels than
were experienced in this study on Ti-6Al-4V. Further work using alpha
type alloys (Reference 12) should help clear this point.

The larger reductions in deformation pressures reported by Kolachev
et al (References 7, 8) up to 0.45 weight percent hydrogen might be
directly attributable to the fact that a greater percentage of the total
metallurgical structure was transforming from the stronger hcp alpha to

the lower strength bcc beta. The large reductions in tensile strength reported for the Ti-5Zr-9Al-5Sn-2Mo (Reference 7), Figure 2, however, require more than an alpha-to-beta structure explanation and perhaps the superplasticity explanation advanced by Kolachev et al (Reference 7) does come into play.

The maximum deformation pressure reductions found in this effort amount to approximately 30 percent of the pressure for non-hydrogenated stock. This amount is about the same as that found by Birla and DePierre (Reference 9) for hydrogenated Ti-6Al-2Sn-4Zr-6Mo.

It is also important to note that since powder produced by the hydride-dehydride process might be expected to contain 2.0 weight percent or more hydrogen, the direct consolidation of hydrided powder would be expected to require higher deformation pressures than would the consolidation of non-hydrogenated powder. This would prove to be a distinct disadvantage for the process unless controlled vacuum hot pressing techniques were utilized and reduction of the hydrogen content to approximately 0.4 weight percent was accomplished before consolidation.

2. EFFECTS OF PROCESS TEMPERATURE

The variation of deformation flow stress with processing temperature can be determined from Figures 6 through 11 for both the $1.26 \times 10^{-4} ms^{-1}$ (.3 ipm) and $1.26 \times 10^{-2} ms^{-1}$ (30 ipm) deformation rates. This information is replotted in Figure 24 for the non-hydrogenated material and for material with 0.4 weight percent hydrogen.

The reduction in flow strength with increasing temperature for the non-hydrogenated material reflects the normal flow softening expected from the alpha to beta transformation. While the beta transus of the non-hydrogenated material would be expected to occur between 1296°K (1825°F) and 1283°K (1850°F) the rate of reduction would be expected to slow appreciably at temperatures higher than 1144°K (1600°F) because of the tendency for plastic deformation to occur in the beta phase with the mostly elongated primary alpha acting as somewhat widely spaced non-deforming hard cylindrical particles.

19

It is notable that the reduction in flow stress with increasing temperature of the alloy containing 0.4 weight percent hydrogen seems to parallel that of the non-hydrogenated material but at a 56°K (100°F) to 83°K (150°F) lower temperature. This effect is similar for both deformation rates.

Information of value from this effect is applicable to isothermal forging processes in that equivalent die loads for processing hydrogenated material can be expected at a 83°K (150°F) lower temperature. This effect can be translated to lower cost and more machinable die materials for isothermal forging.

3. EFFECT OF TRANSFORMATION PRECONDITIONING

Transformation preconditioning of hydrogenated material has little effect on deformation resistance of the material. The effect which was noted was slightly increased initial deformation stresses when the material was exposed to temperature in the beta range. This effect is probably attributable to the high strength of the large beta grains.

4. EFFECT OF HEAT-TO-HEAT

Material variations likewise showed only a minimal effect at the start of deformation where the microstructural morphology difference would be expected to have larger contributions.

SECTION VI

CONCLUSIONS

The analysis of the data developed for this report allows the following conclusions to be made.

1. The flow stress of hydrogenated Ti-6Al-4V alloys is reduced with increased hydrogen content up to approximately 0.4 weight percent hydrogen. At this hydrogen concentration, the flow stress reduction is approximately 30 percent of that of non-hydrogenated material. Hydrogen levels greater than 0.4 weight percent cause a corresponding increase in the flow stress. When approximately 0.8 weight percent hydrogen is added, the flow stress is about equal to that of non-hydrogenated product. The increase in deformation flow stress at hydrogen levels greater than 0.4 weight percent is attributable to the occurrence of the gamma phase in the microstructure.

2. The deformation pressures for processing of materials with 0.4 weight percent hydrogen are equivalent to those for non-hydrogenated material at a temperature approximately 56°K (100°F) to 83°K (150°F).

3. Transformation preconditioning and heat-to-heat variations play only a small role on deformation flow stress.

TABLE 1

COMPARISON OF HYDROGEN ANALYSIS TECHNIQUES

SPECIMEN NUMBER	HYDROGEN CONTENT IN WEIGHT PERCENT BY WEIGHT GAIN	BY VACUUM FUSION	PERCENT* DIFFERENCE
221	.346	.391	+ +13%
360	.744	.744	0
367	.738	.720	-2.5%
406	.447	.440	-1.6%
535	.930	1.015	+9.1%
536	.922	.940	+2.0%
615	.729	.757	+3.7%
643	.907	.950	+4.7%
D-16	.894	.920	+2.8%
D-20	.912	.940	+3.1%
D-21	.903	.909	+0.7%
D-24	.907	.904	-0.2%

*Based on weight gain technique

TABLE 2

COMPARISON OF HYDROGEN CONTENT BY WEIGHT GAIN AND WEIGHT LOSS

SPECIMEN NUMBER	WEIGHT GAIN IN PERCENT	WEIGHT LOSS IN PERCENT	PERCENT DIFFERENCE	RESIDUAL H_2 BY VAC. FUSION IN PPM
T-1	.463	.455	.008	8
T-5	.496	.484	.012	5
T-8	.474	.465	.009	5
T-10	.494	.478	.014	3
		AVG.	.011%	

TABLE 3

WEIGHT GAIN AND LOSS BY SAMPLES ON HYDROGENATION AND DEHYDROGENATION CYCLES WITHOUT HYDROGEN CONTAINING GAS

SPECIMEN NUMBER	WEIGHT GAIN IN PERCENT	WEIGHT LOSS IN PERCENT	RESIDUAL H_2 BY VAC. FUSION IN PPM
T-13	.001	.002	22
T-15	.0	.014	6
T-17	.001	.008	3
T-19	.0	.014	3
	AVG.	.010%	

TABLE 4

HYDROGEN RETENTION DATA

TEMPERATURE °K (°F)	TIME (Hrs.)	COATING	SPECIMEN THICKNESS (Inches)	PERCENT HYDROGEN Retained
1033 (1400)	1/2	None	1/8	96.0
			1/4	98.2
			1/2	97.6
1033 (1400)	1/2	Frit	1/8	98.7
			1/4	98.6
			1/2	99.2
1033 (1400)	1/2	Fused	1/8	93.8
			1/4	98.7
			1/2	98.2
1144 (1600)	1/2	None	1/8	89.1
			1/4	93.3
			1/2	96.4
1044 (1600)	1/2	Frit	1/8	98.2
			1/4	98.7
			1/2	98.7
1144 (1600)	2	Fused	1/8	98.5
			1/4	99.3
			1/2	98.8
1144 (1600)	4	Frit	1/8	97.7
			1/4	98.7
			1/2	99.1
1144 (1600)	4	None	1/8	100.5
			1/4	83.0
			1/2	90.5
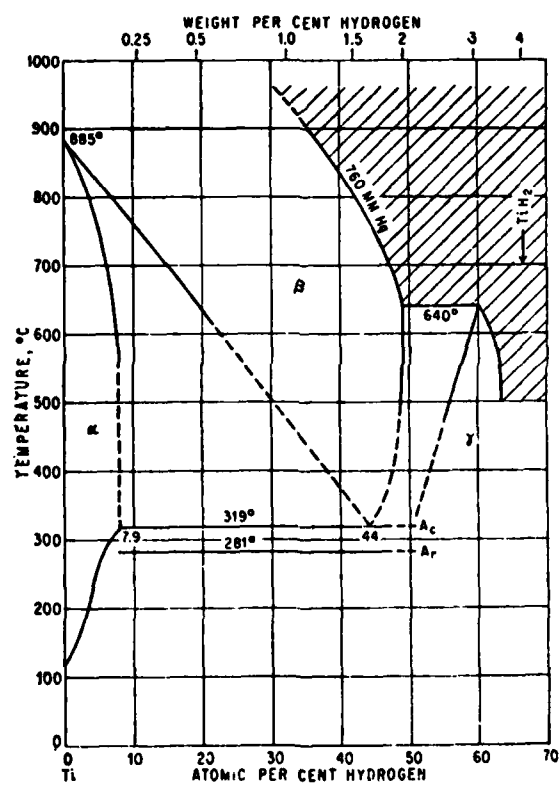
Figure 1. Phase Relation Between Titanium
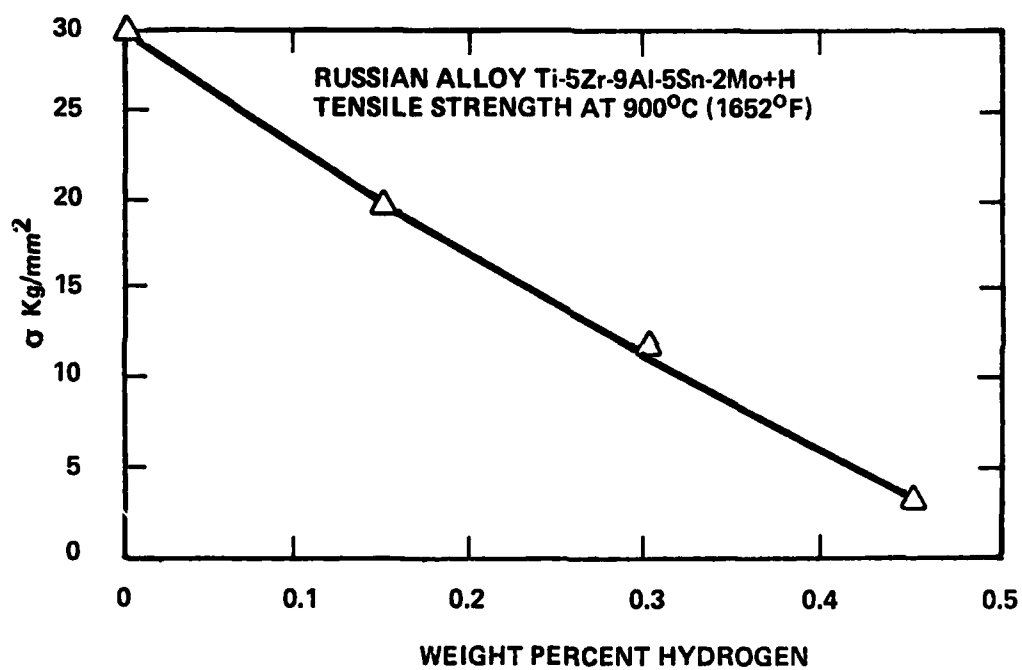and Hydrogen

Figure 2. Tensile Strength of Ti-5Zr-9Al-5Sn-2Mo at 1173°K
as a Function of Hydrogen Content
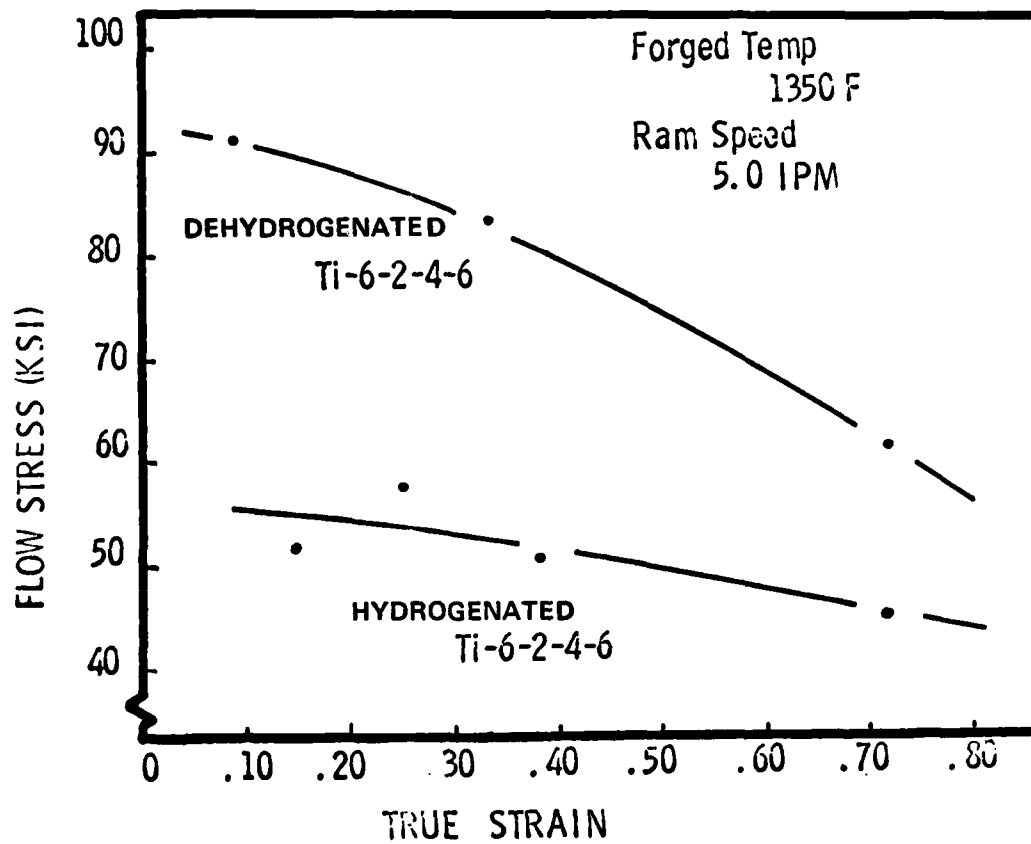
Figure 3. Comparison of Flow Stress of Hydrogenated and
Non-hydrogenated Ti-6Al-2Sn-4Zr-6Mo as a
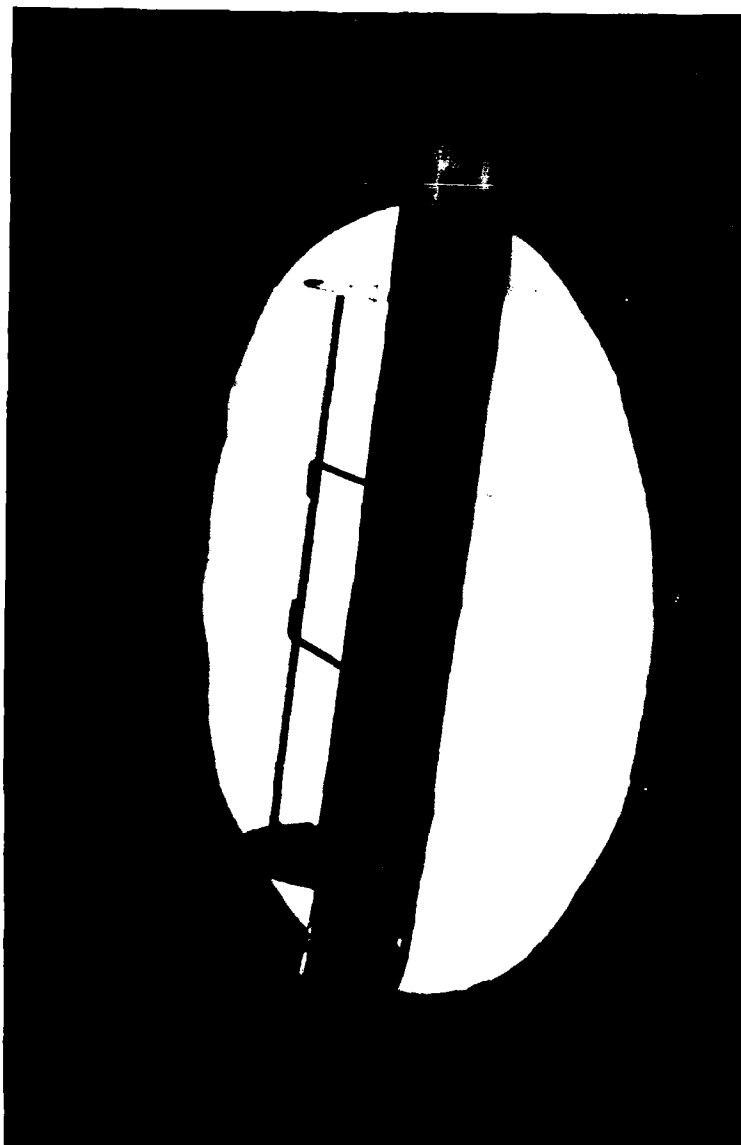Function of Strain

27

Figure 4. Hydrogenation Equipment

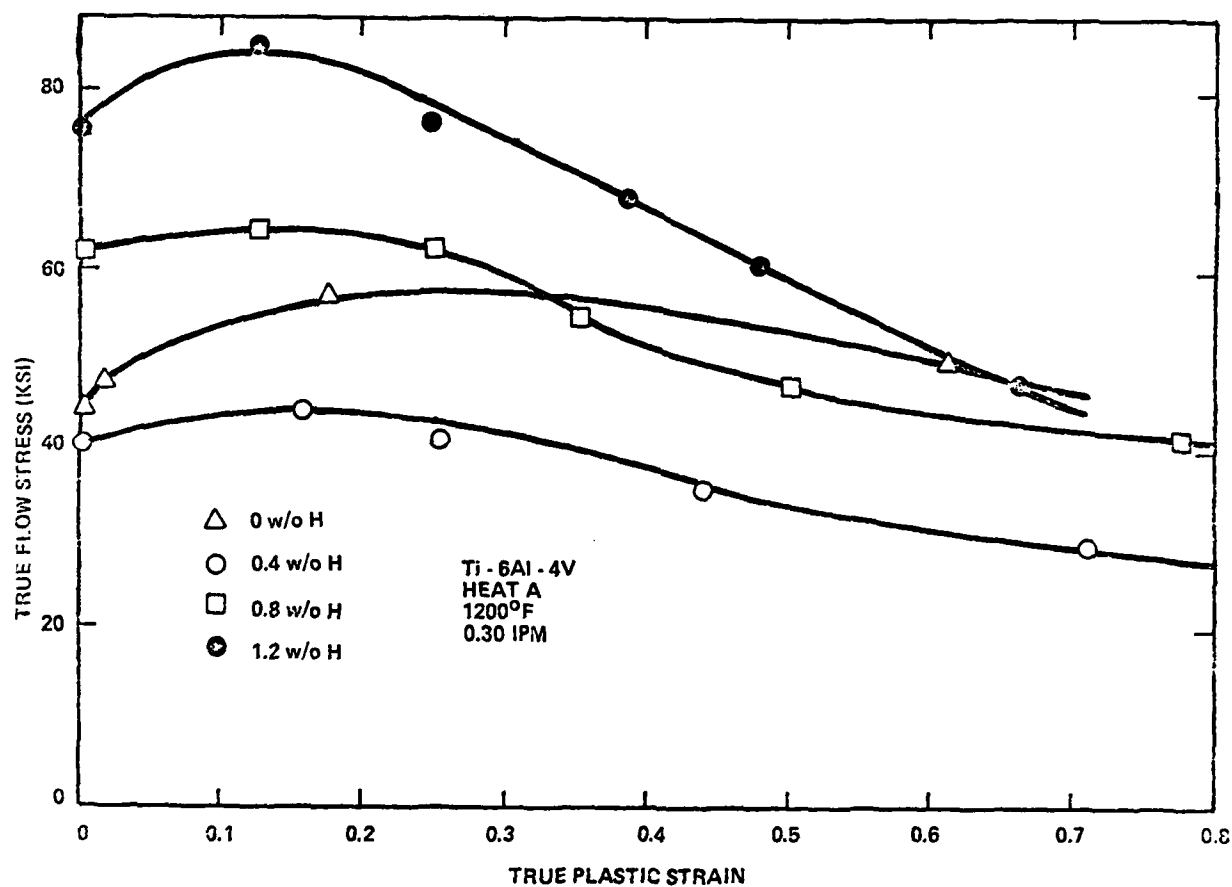Figure 5. Rack used to Hold Specimens During Hydrogenation

Figure 6. Flow Stress-Plastic Strain Relation for Ti-6Al-4V Alloy (Heat A) with Various Hydrogen Contents Isothermally Forged at 922°K (1200°F) and $1.26 \times 10^{-4} ms^{-1}$ (0.3 ipm)
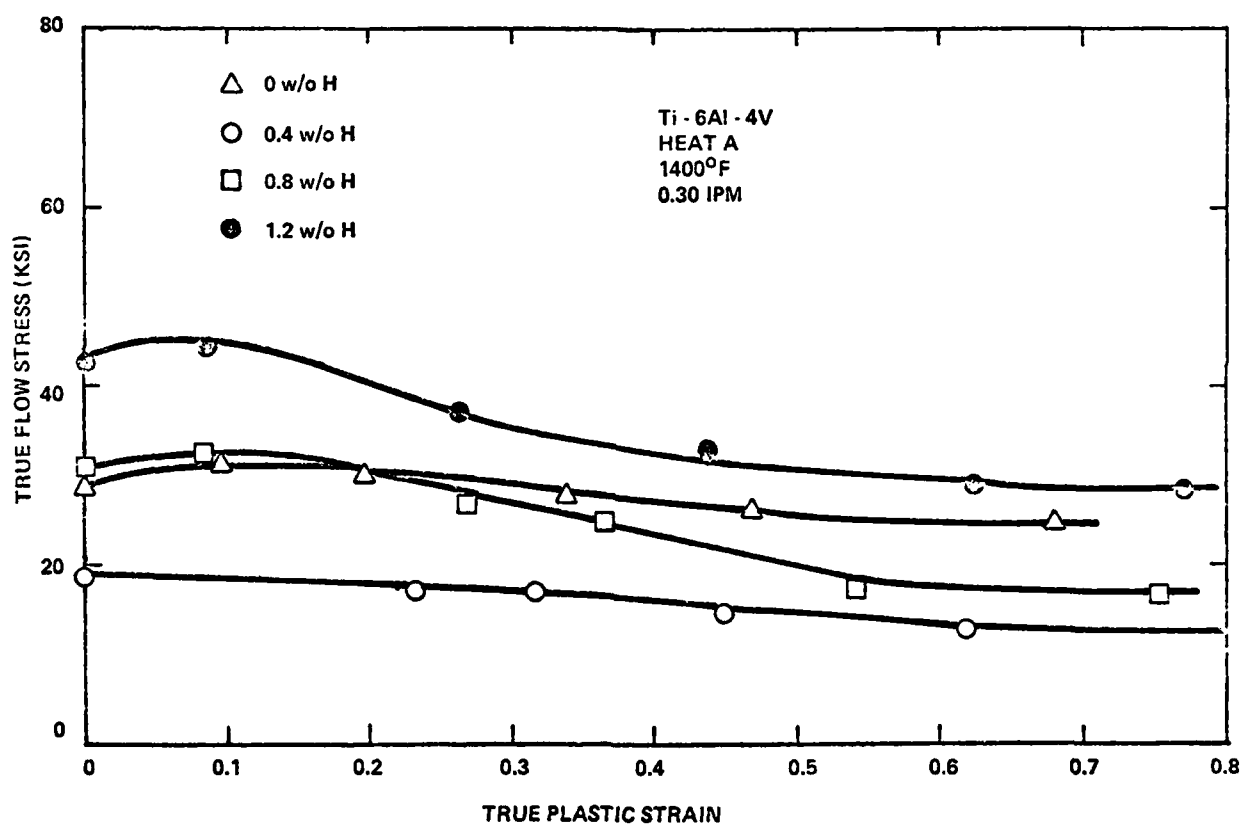
Figure 7.   Flow Stress-Plastic Strain Relation for Ti-6Al-4V Alloy (Heat A)
with Various Hydrogen Contents Isothermally Forged at 1033°K
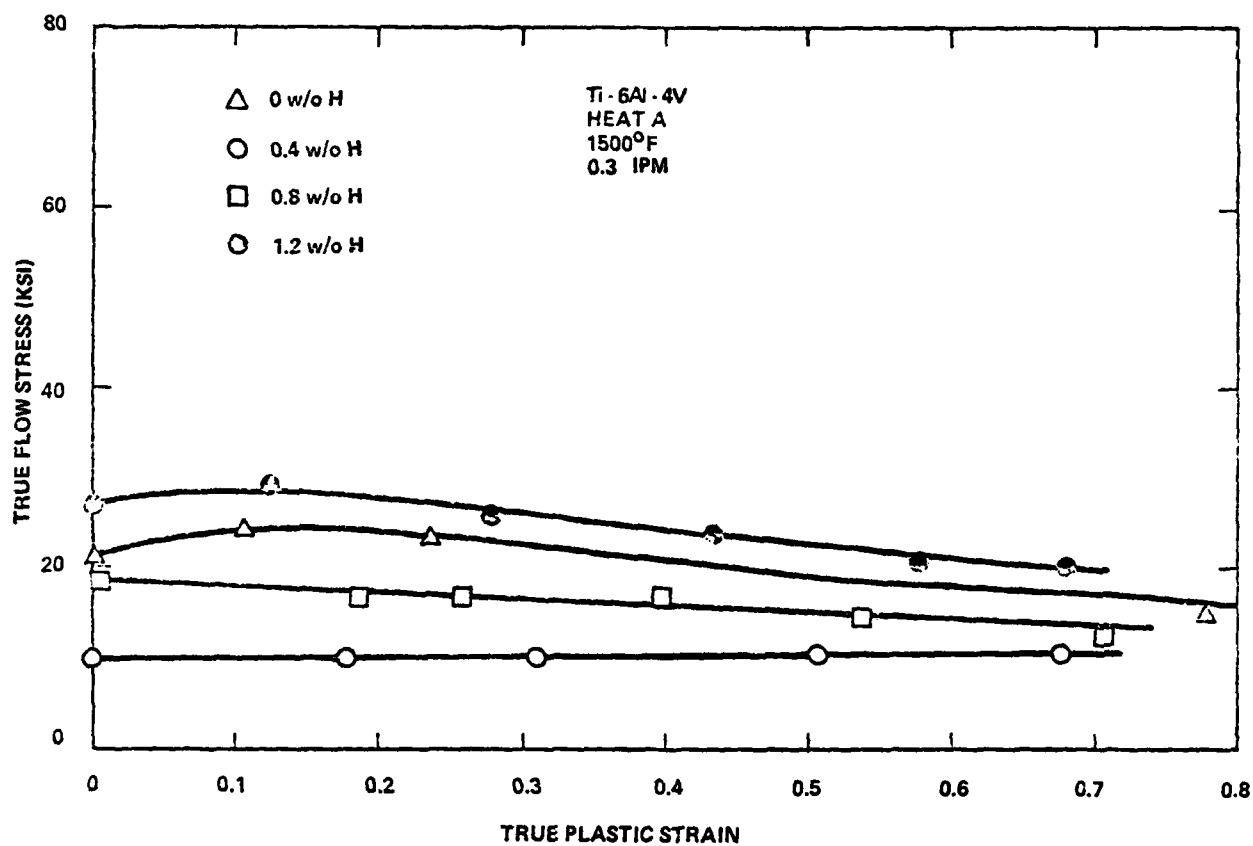(1400°F) and $1.26 \times 10^{-4} ms^{-1}$ (0.3 ipm)

Figure 8. Flow Stress-Plastic Strain Relation for Ti-6Al-4V (Heat A) with Various Hydrogen Contents Isothermally Forged at 1089°K (1500°F) and $1.26 \times 10^{-4} ms^{-1}$ (0.3 ipm)
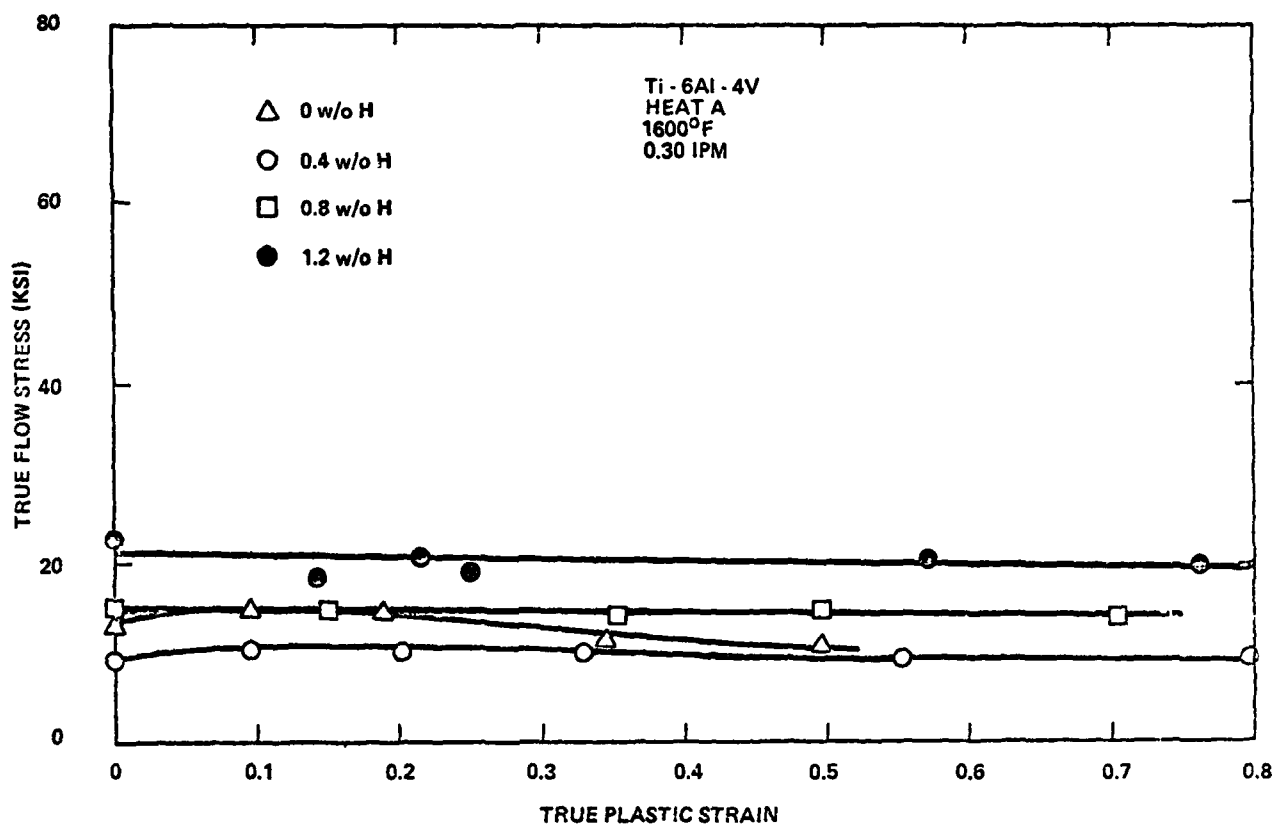
Figure 9. Flow Stress-Plastic Strain Relation for Ti-6Al-4V (Heat A) with Various Hydrogen Contents Isothermally Forged at 1144°K (1600°F) and $1.26 \times 10^{-4} \text{ms}^{-1}$ (0.3 ipm)

Figure 10. Flow Stress-Plastic Strain Relation for Ti-6Al-4V (Heat A) with Various Hydrogen Contents Isothermally Forged at 1033°K (1400°F) and $1.26 \times 10^{-2} ms^{-1}$ (30.0 ipm)
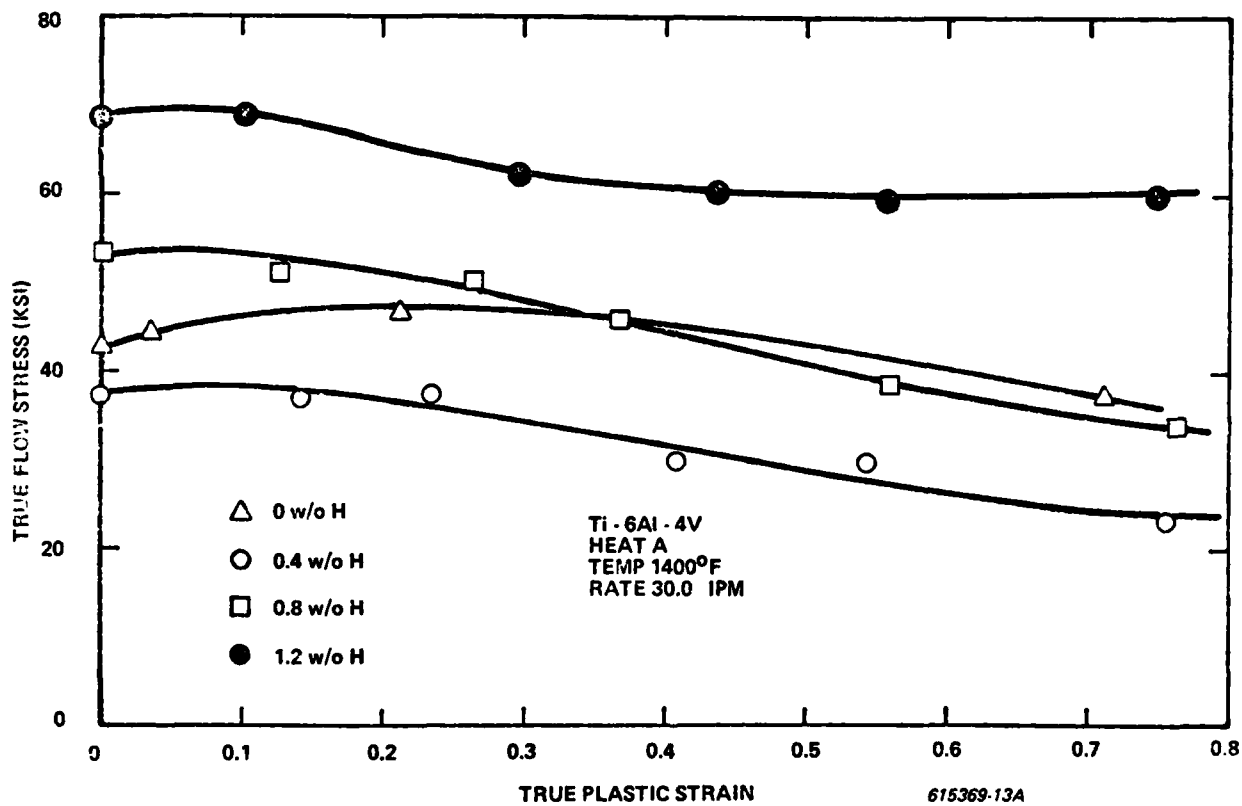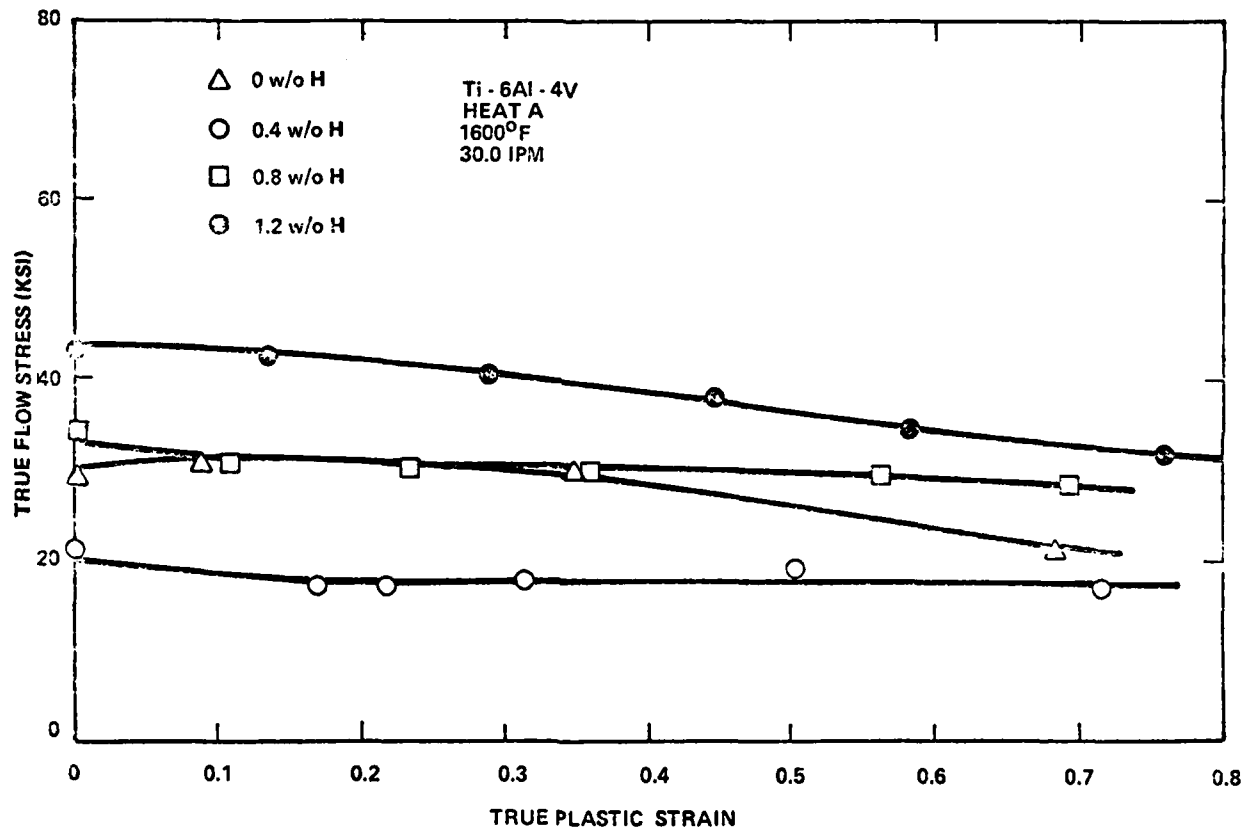
Figure 11.   Flow Stress-Plastic Strain Relation for Ti-6Al-4V (Heat A) with
Various Hydrogen Contents Isothermally Forged at 1144°K (1600°F)
and $1.26 \times 10^{-2} ms^{-1}$ (30.0 ipm)
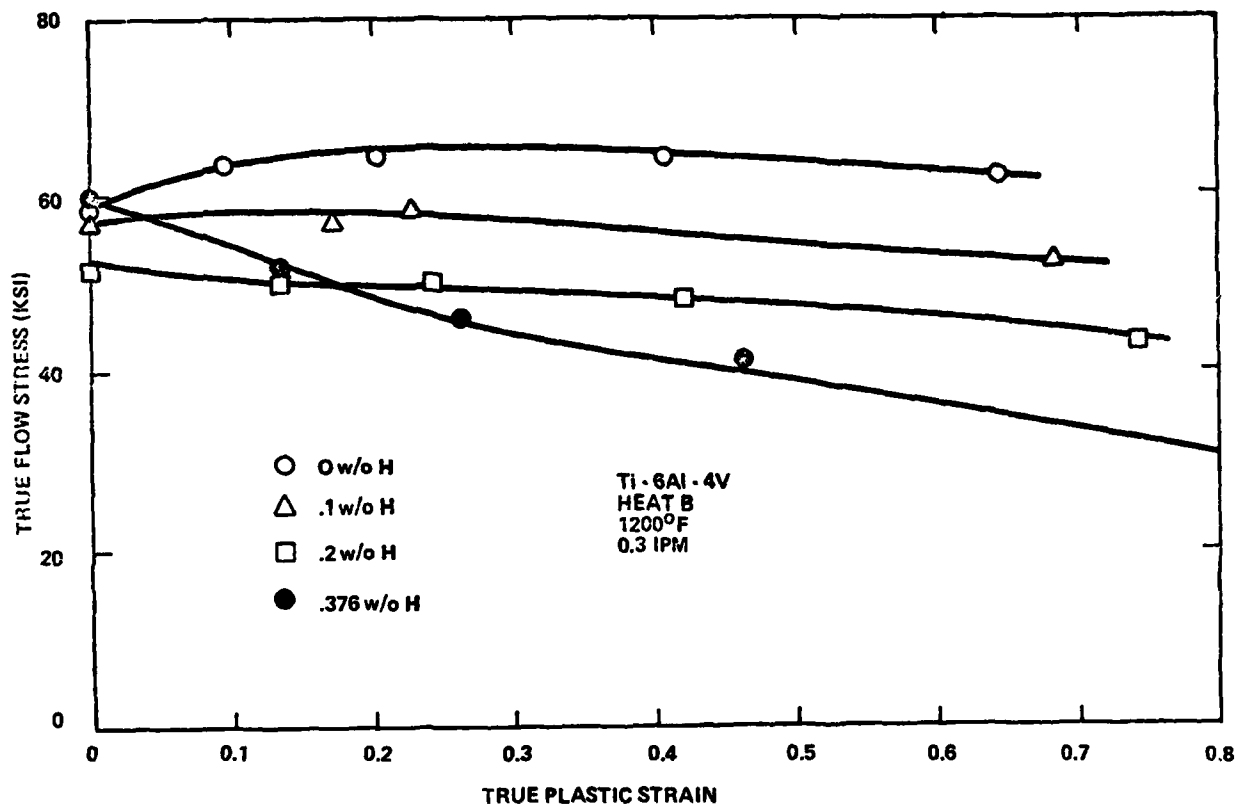
Figure 12. Flow Stress-Plastic Strain Relation for Ti-6Al-4V (Heat B) with Various Hydrogen Contents Isothermally Forged at 922°K (1200°F) and $1.26 \times 10^{-4} ms^{-1}$ (0.3 ipm)

Figure 13. Flow Stress-Plastic Strain Relation for Ti-6Al-4V (Heat B) with Various Hydrogen Contents Isothermally Forged at 1033°K (1400°F) and $1.26 \times 10^{-4} ms^{-1}$ (0.3 ipm)

Figure 14. Flow Stress-Plastic Strain Relation for Ti-6Al-4V (Heat B) with
Various Hydrogen Contents Isothermally Forged at 1033°K (1400°F)
and $1.26 \times 10^{-2} ms^{-1}$ (30.0 ipm)
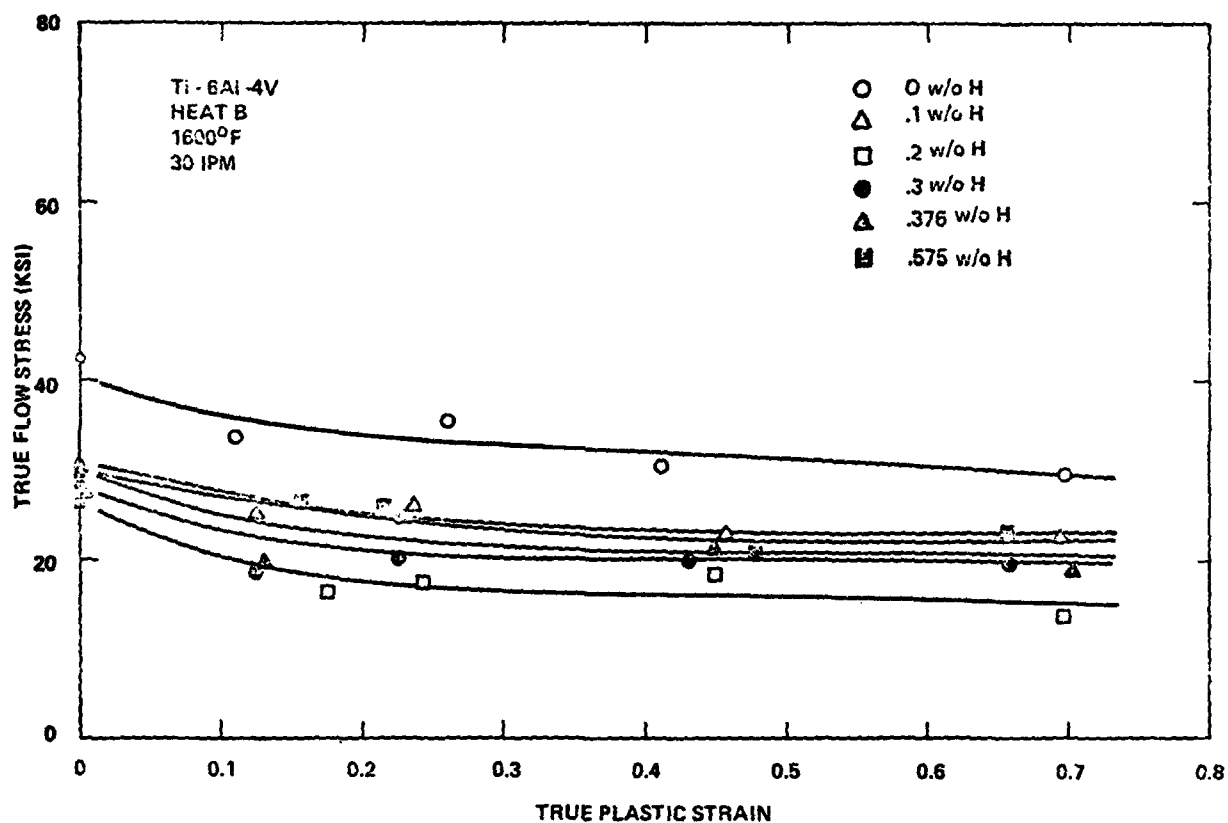
Figure 15. Flow Stress-Plastic Strain Relation for Ti-6Al-4V (Heat B) with Various Hydrogen Contents Isothermally Forged at 1144°K (1600°F) and $1.26 \times 10^{-2} ms^{-1}$ (30.0 ipm)

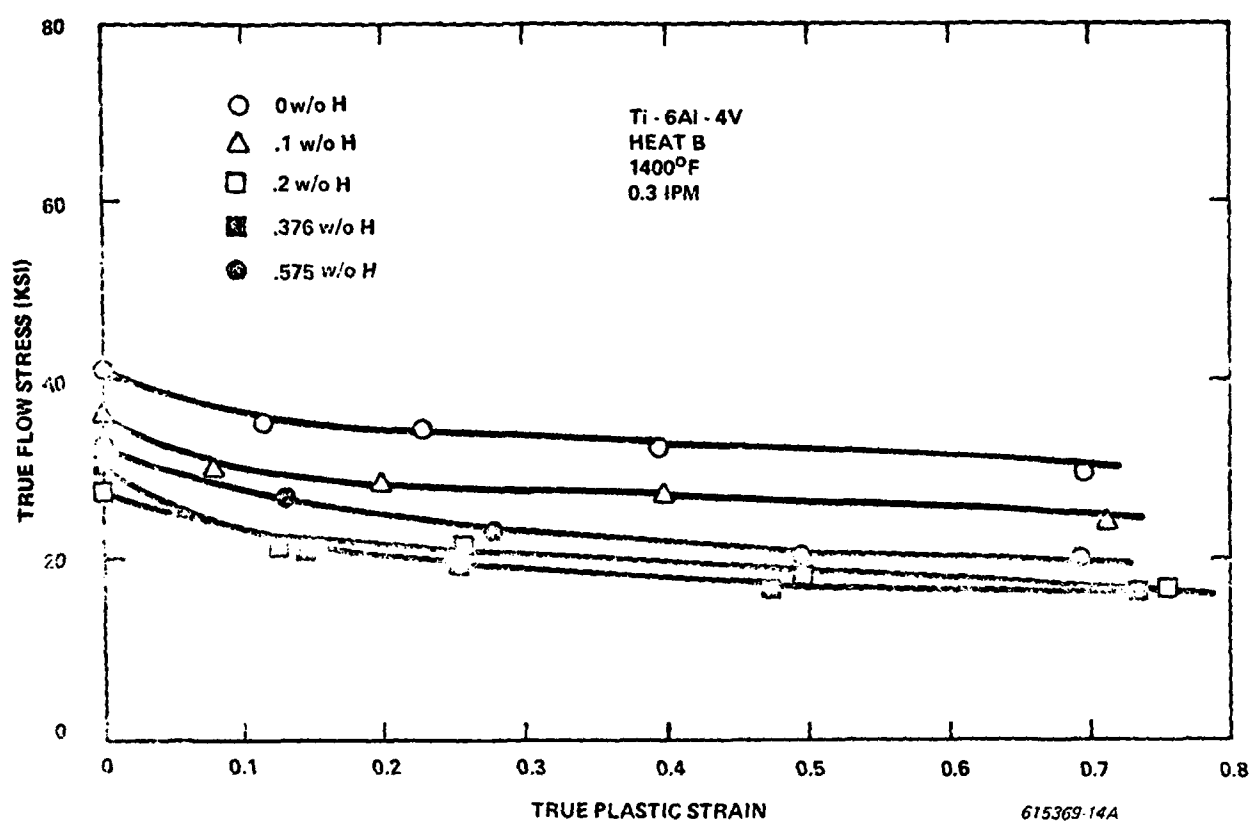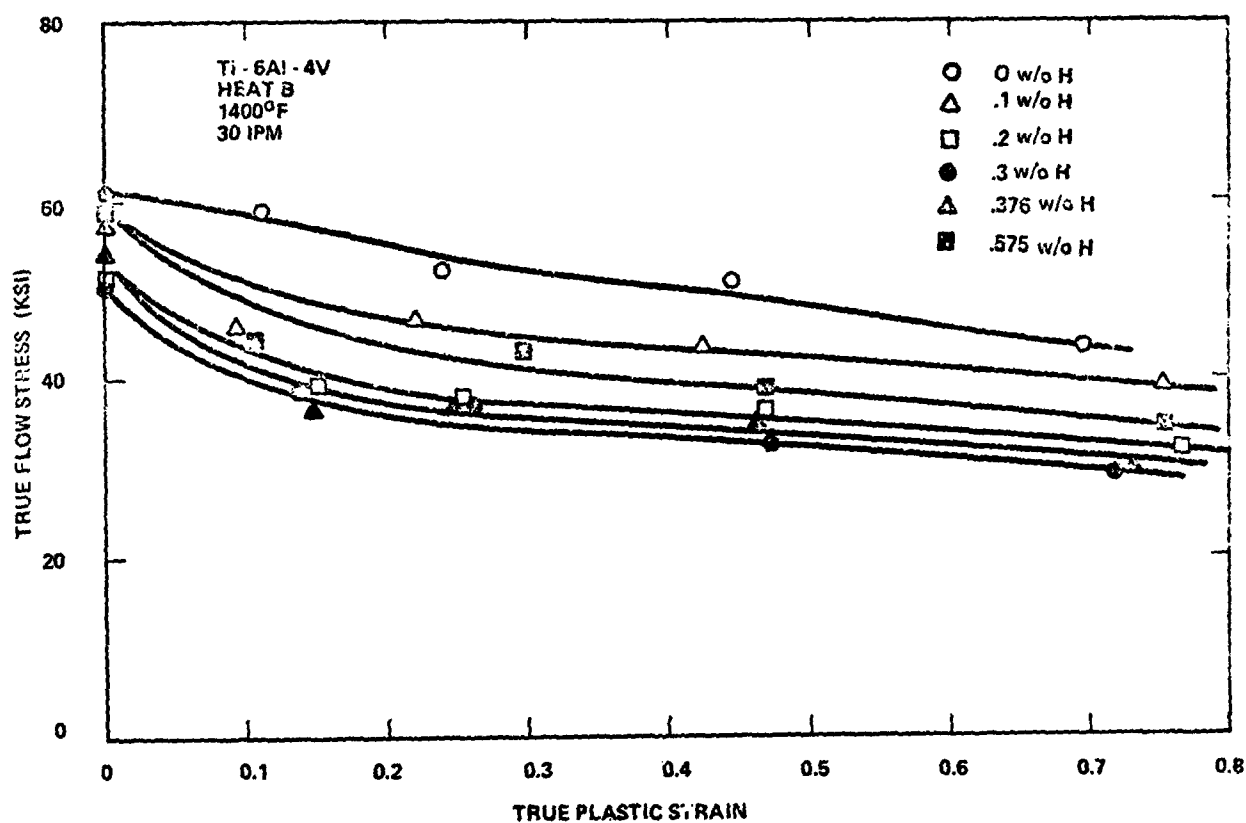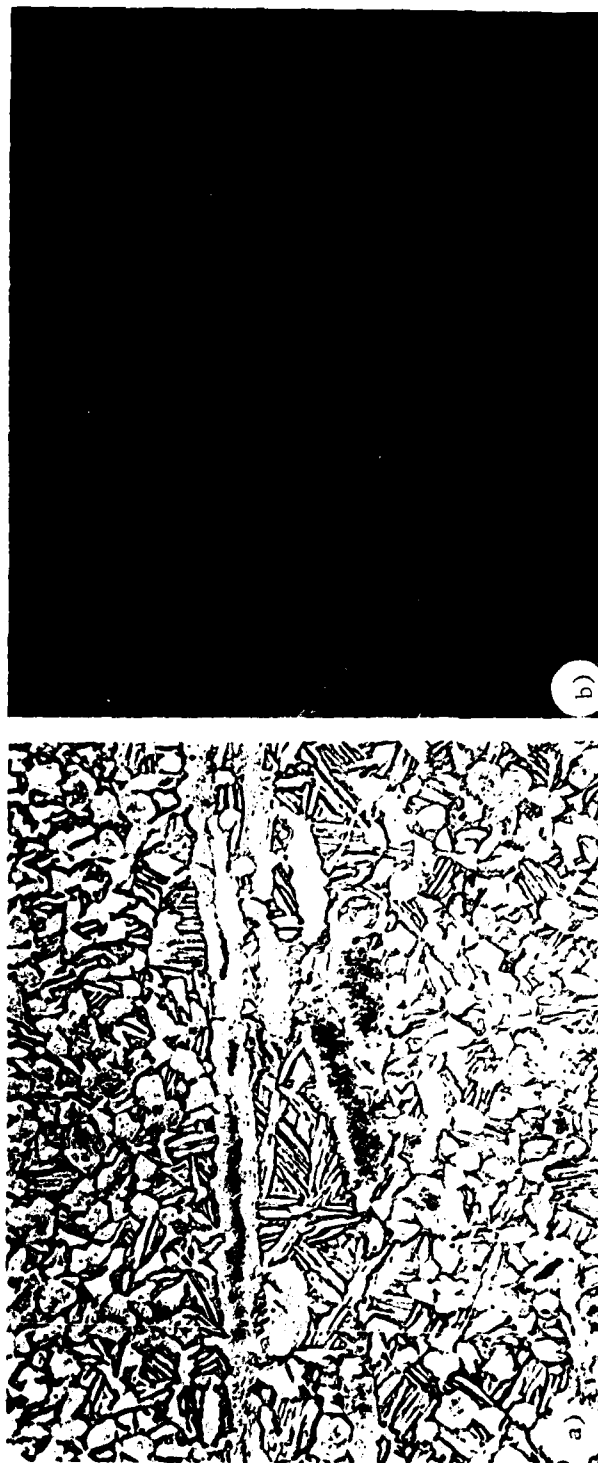Figure 16. Microstructural Effects of Hydrogen Content on the Product from (Heat B) Forged at 1144°K (1600°F) at $1.26 \times 10^{-2} ms^{-1}$ (30.0 ipm), a) 0 w/o H, b) 0.1 w/o H, c) 0.2 w/o H, d) 0.3 w/o H, e) 0.376 w/o H, and f) 0.575 w/o H
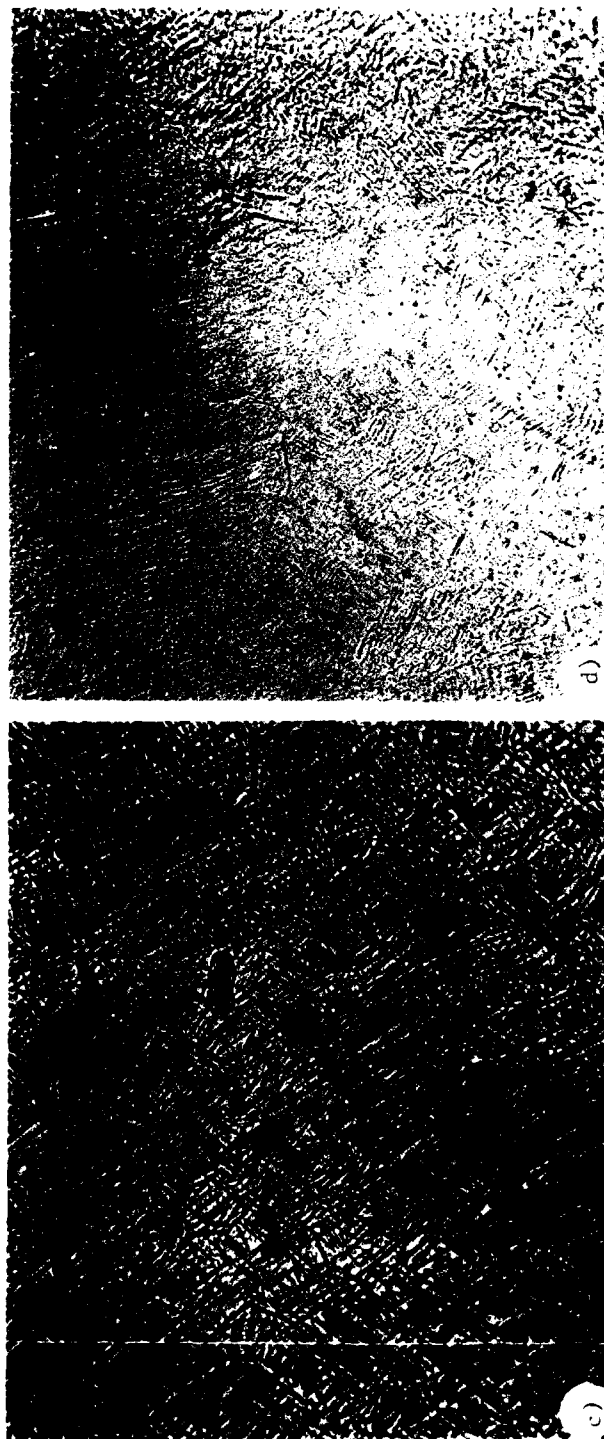
Figure 16. (Continued)

Figure 16. (Continued)

Figure 17. Flow Stress-Plastic Strain Relation for Ti-6Al-4V (Heat B) with 0.4 Weight Percent Hydrogen which was Beta Temperature Exposed Prior to Forging Compared with Material Similarly Treated but Dehydrogenated Prior to Forging. Forged Isothermally at 922°K (1200°F) with a Ram Velocity of of 1.26×10^{-4} ms^{-1} (0.3 ipm)

Figure 18. Flow Stress-Plastic Strain Relation for Ti-6Al-4V (Heat B) with 1.2 Weight Percent Hydrogen which was Beta Temperature Exposed Prior to Forging Compared with Material Similarly Treated but Dehydrogenated Prior to Forging. Forged Isothermally at 922°K (1200°F) with a Ram Velocity of $1.26 \times 10^{-4} ms^{-1}$ (0.3 ipm)
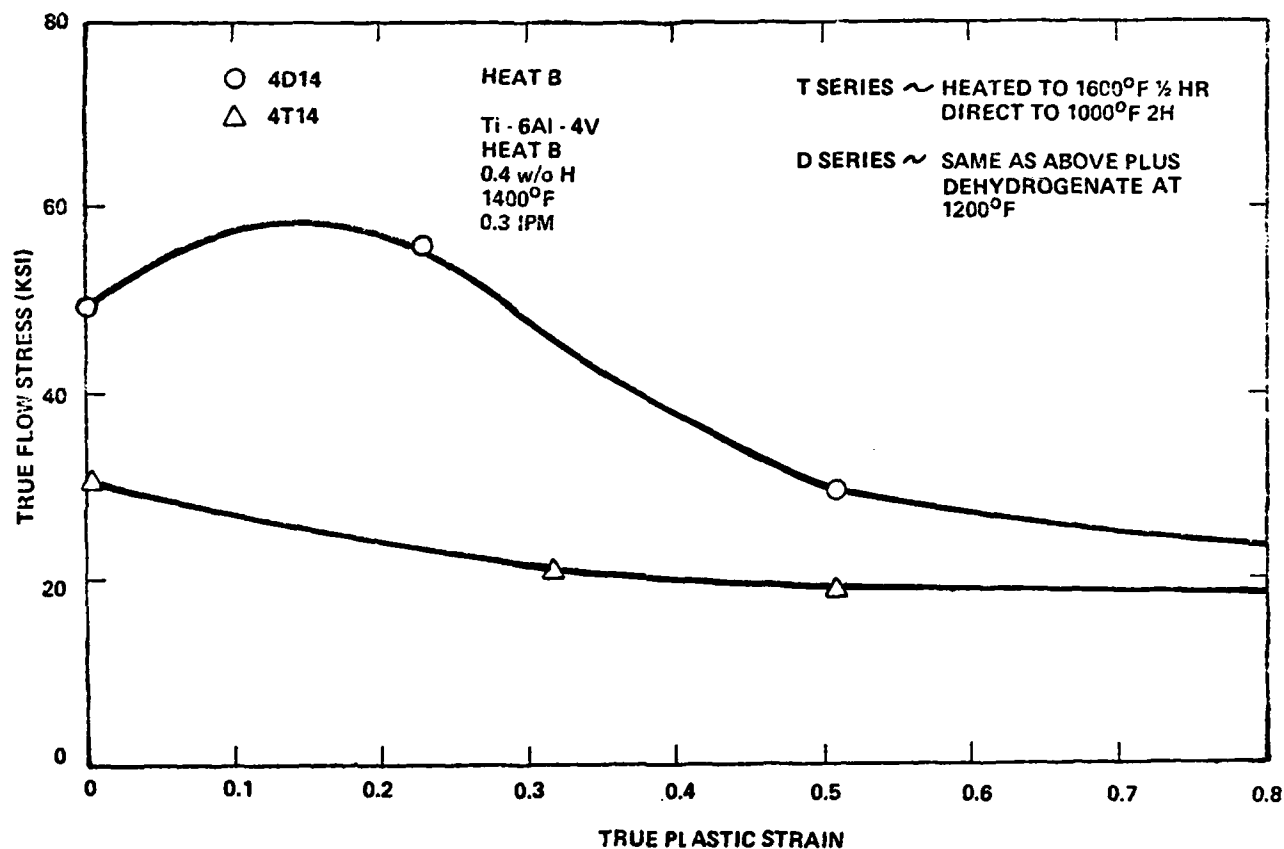
Figure 19. Flow Stress-Plastic Strain Relation for Ti-6A1-4V (Heat B) with 0.4 Weight Percent Hydrogen which was Beta Temperature Exposed Prior to Forging Compared with Material Similarly Treated but Dehydrogenated Prior to Forging. Forged Isothermally at 1033°K (1400°F) with a Ram Velocity of $1.26 \times 10^{-4} ms^{-1}$ (0.3 ipm)
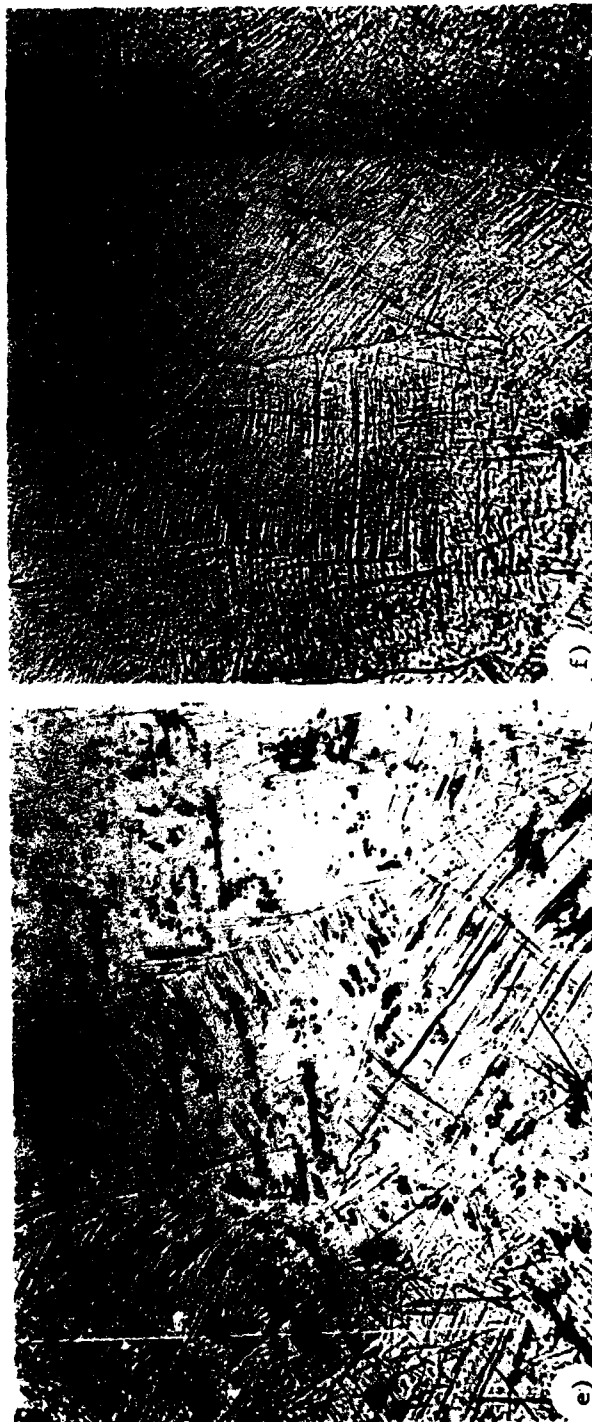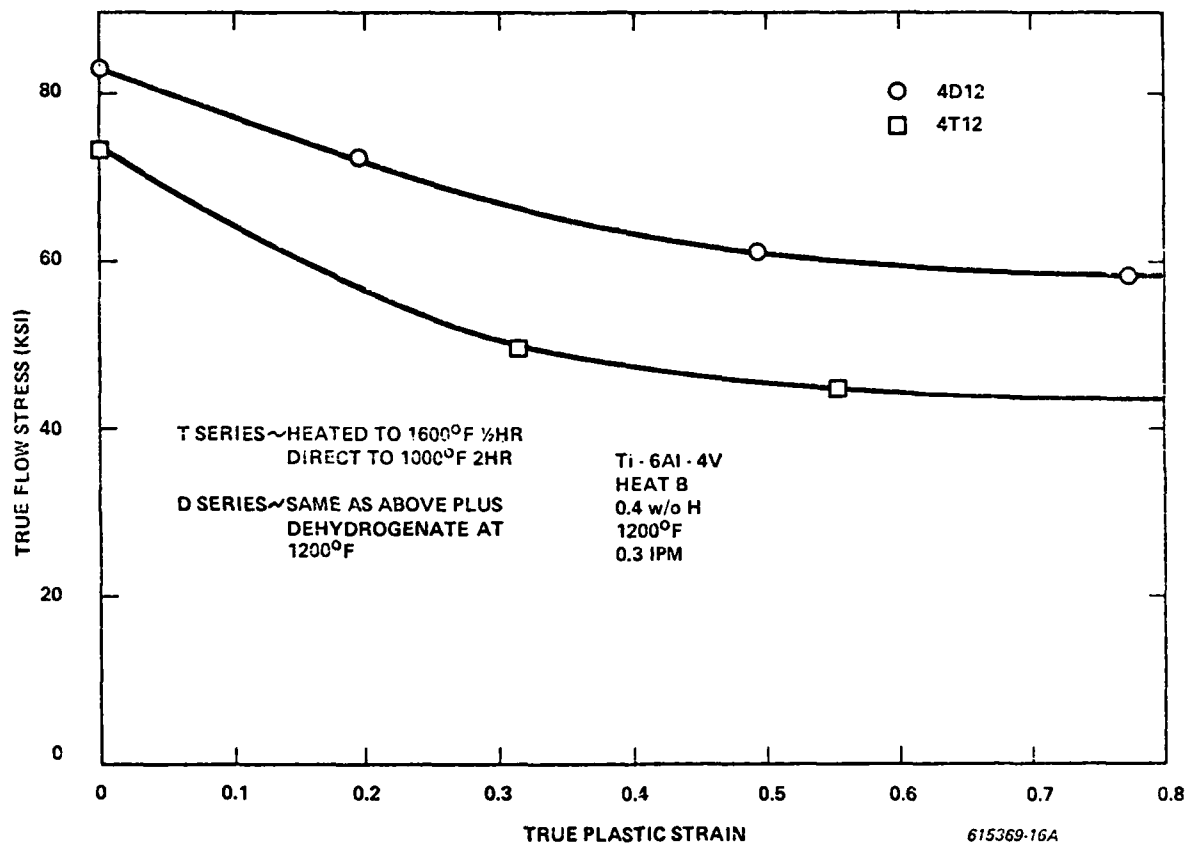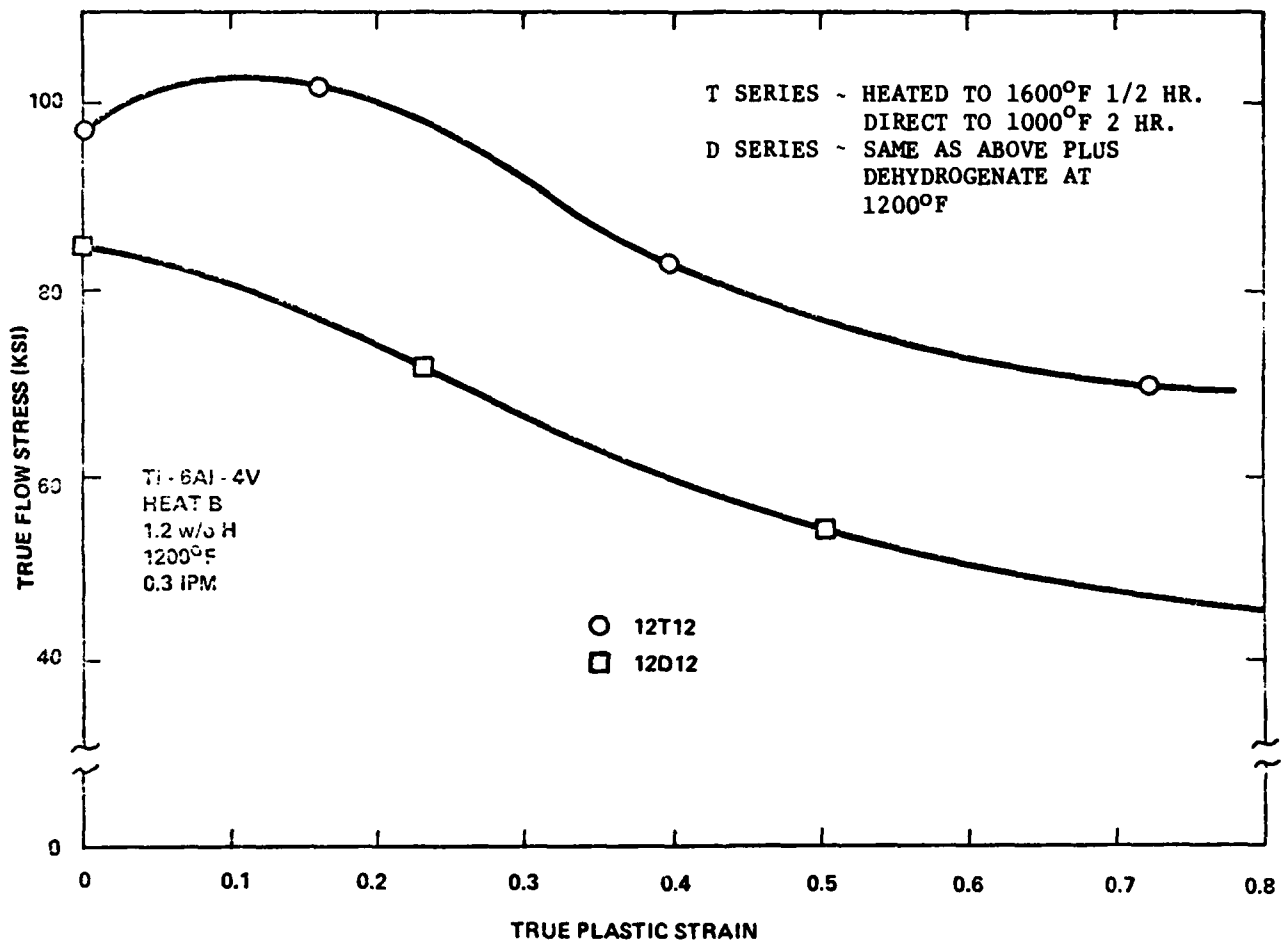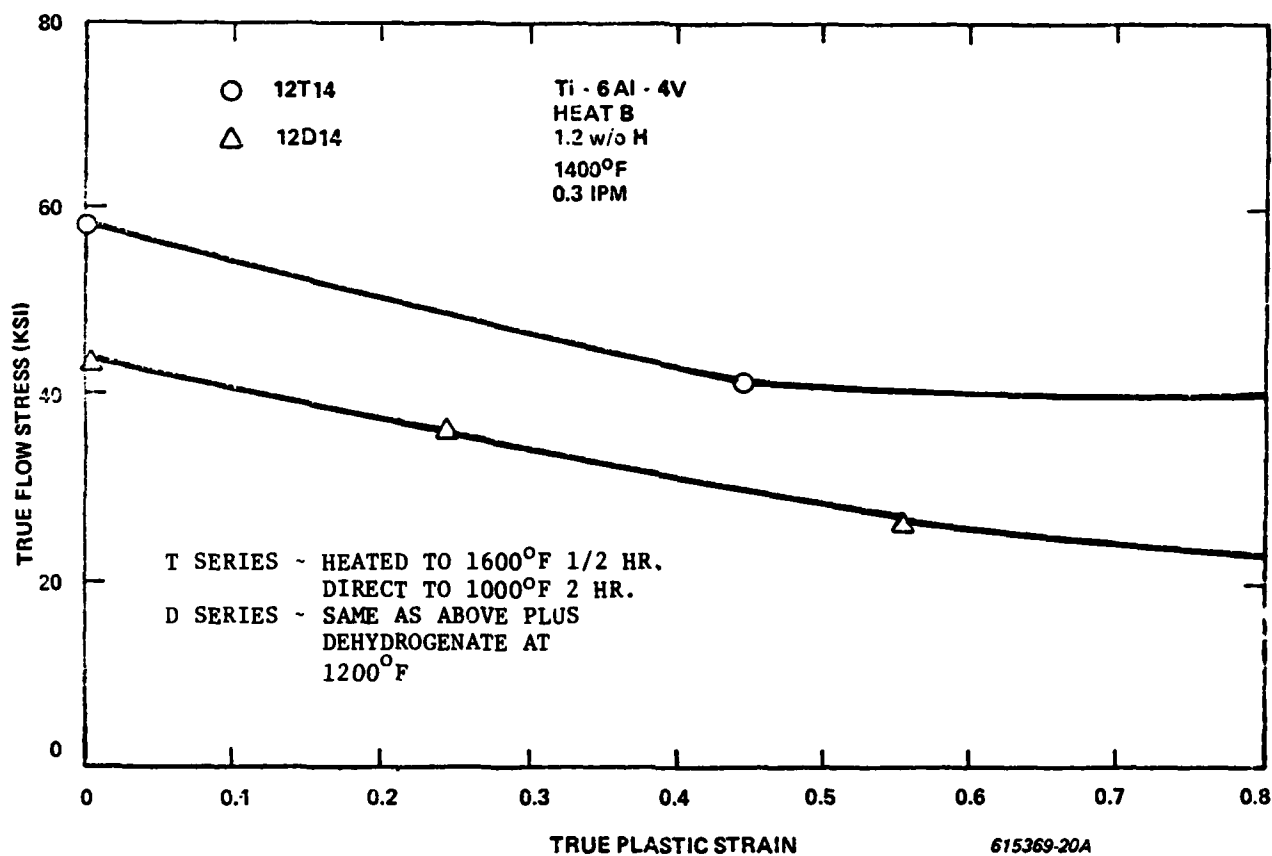
Figure 20. Flow Stress-Plastic Strain Relation for Ti-6Al-4V (Heat B)
with 1.2 Weight Percent Hydrogen which was Beta Temperature
Exposed Prior to Forging Compared with Material Similarly
Treated but Dehydrogenated Prior to Forging. Forged
Isothermally at 1033°K (1400°F) with a Ram Velocity of
$1.26 \times 10^{-4} ms^{-1}$ (0.3 ipm)
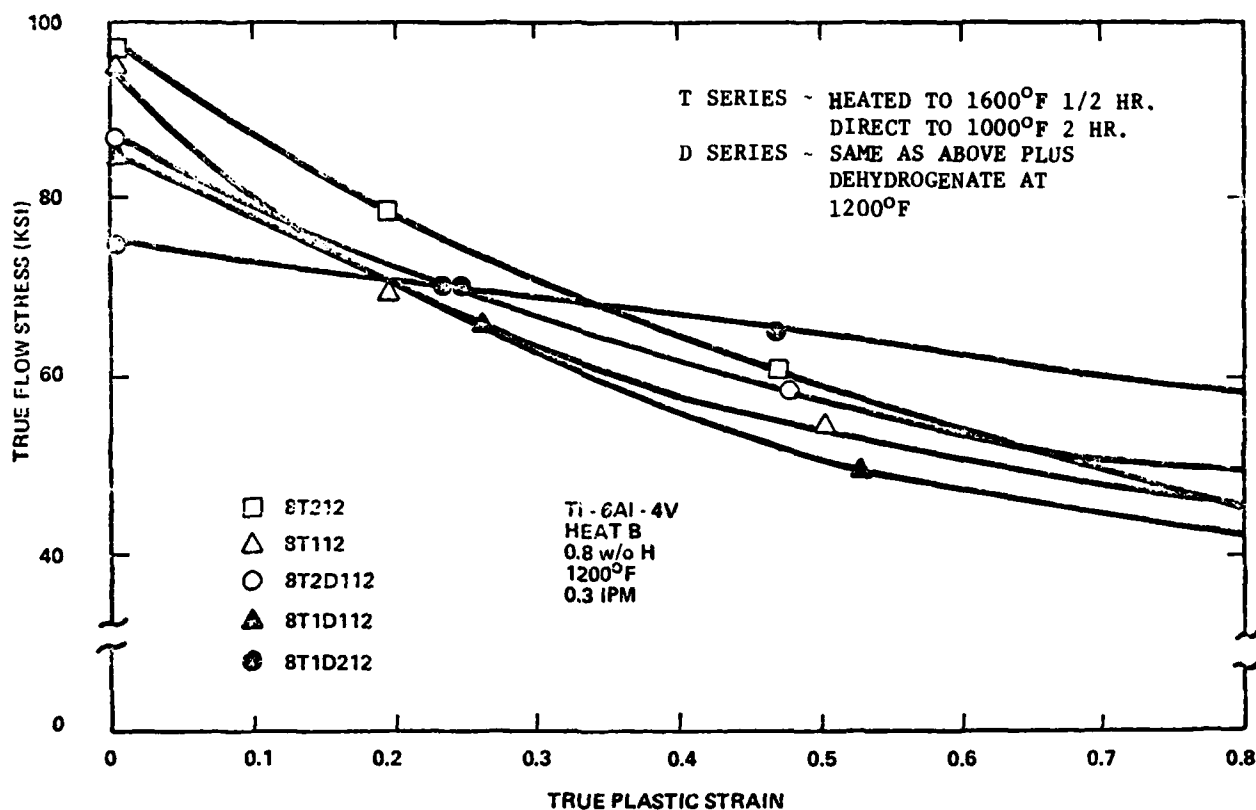
Figure 21. Comparison of the Effect of Various Thermal Cycles on the Flow Stress-Plastic Strain Relation of Ti-6Al-4V (Heat B) with 0.8 Weight Percent Hydrogen. Some Material was Dehydrogenated Prior to Isothermal Forging at 922°K (1200°F) with a Ram Velocity of 1.26×10^{-4} ms^{-1} (0.3 ipm)
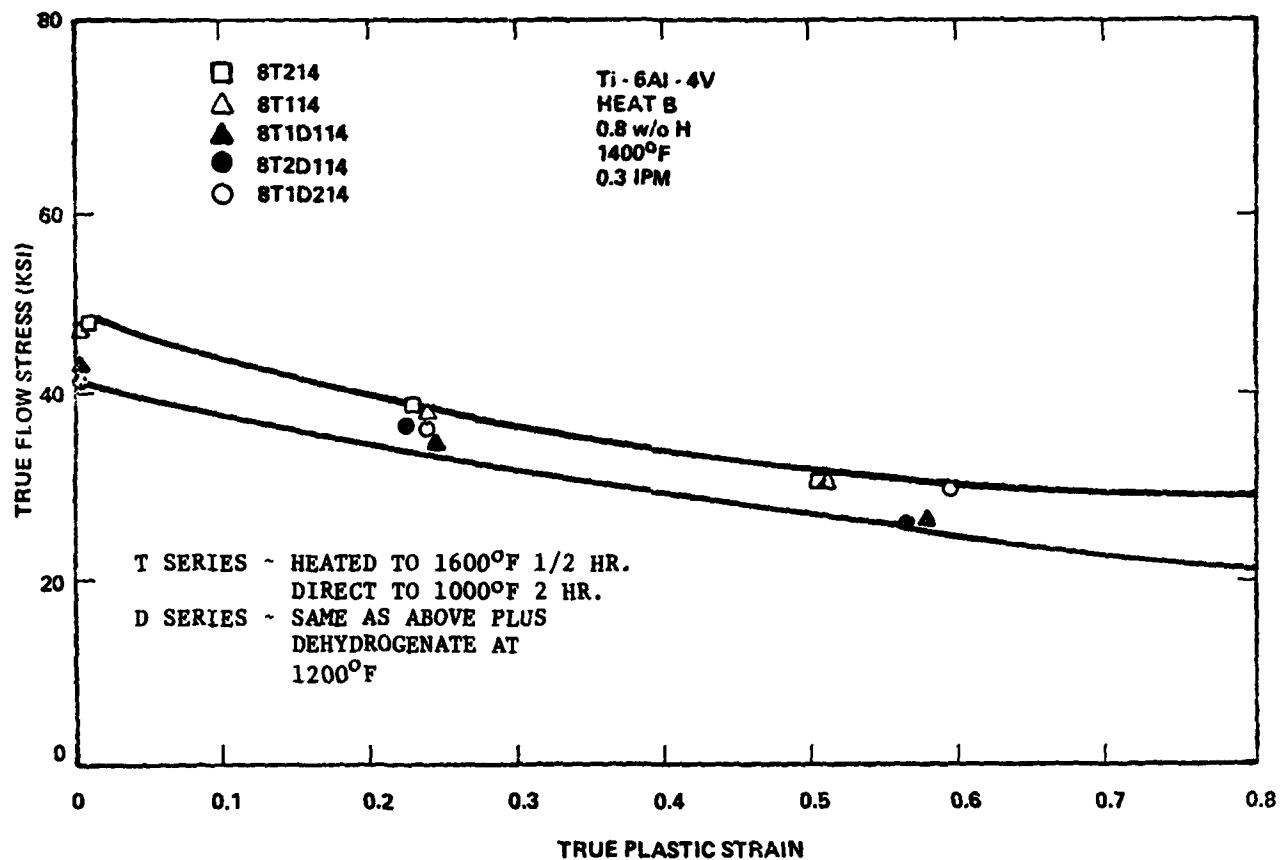
Figure 22. Comparison of the Effect of Various Thermal Cycles on the Flow Stress-Plastic Strain Relation of Ti-6Al-4V (Heat B) with 0.8 Weight Percent Hydrogen. Some Material was Dehydrogenated Prior to Forging Isothermally at 1033°K (1400°F) with a Ram Velocity of $1.26 \times 10^{-4} ms^{-1}$ (0.3 ipm)
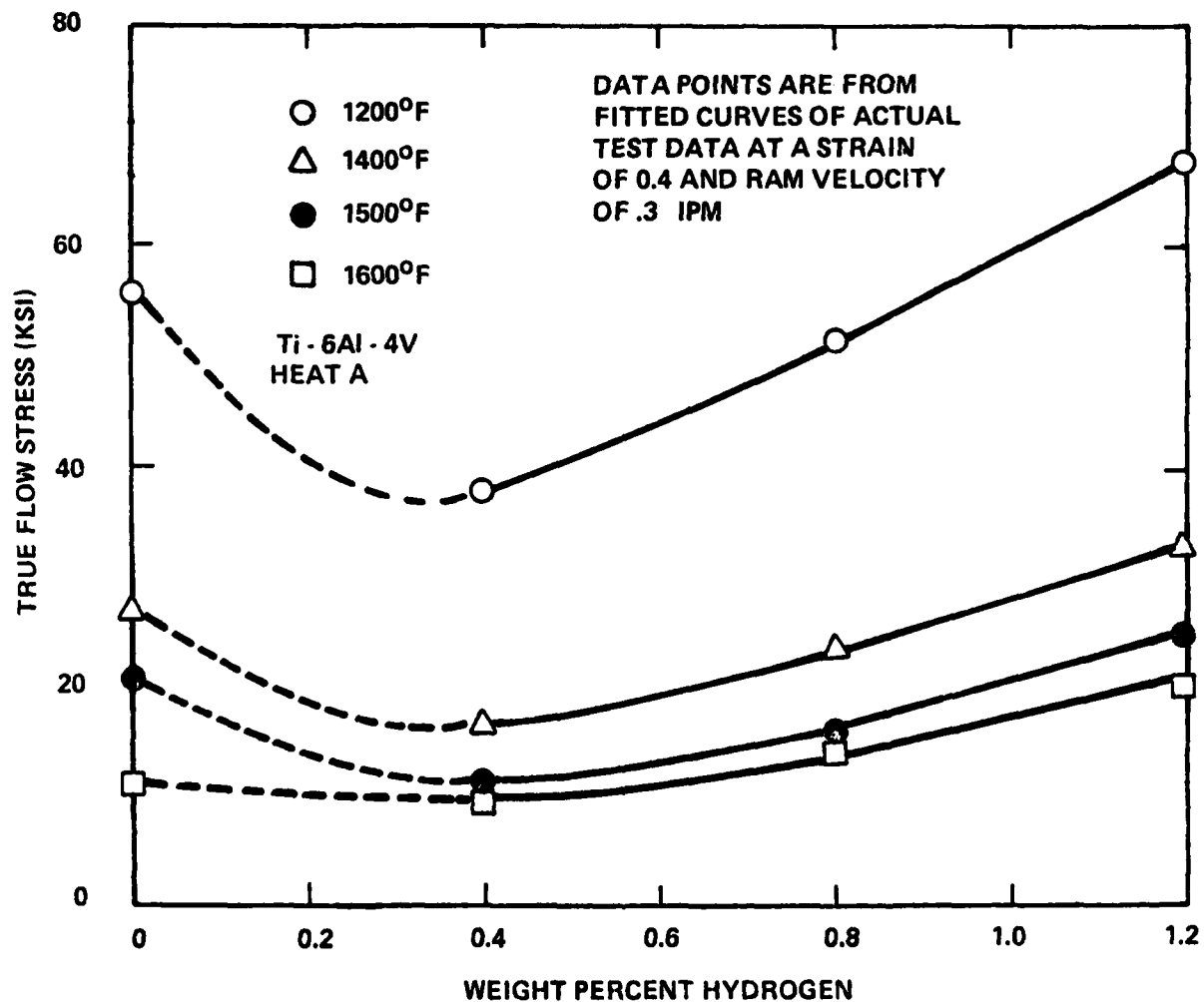
Figure 23. Illustration of the Effects of Hydrogen Concentration on the Peak Deformation Stress of Ti-6Al-4V (Heat A). Material was Isothermally Forged at Various Temperatures using a Ram Velocity of 1.26×10^{-4} ms^{-1} (0.3 ipm)
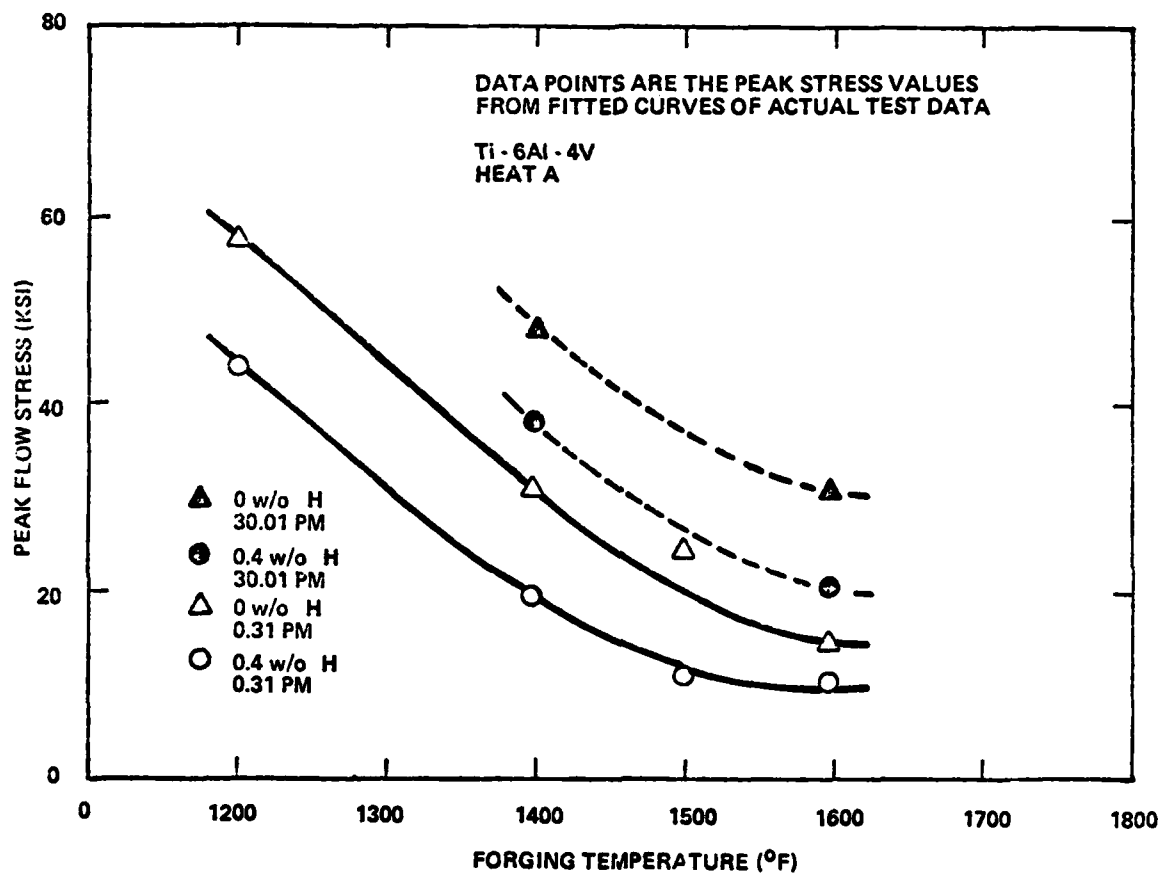
Figure 24.   Illustration of the Effects of Forging Temperature on Flow
Stress of Non-Hydrogenated Material and Material Hydrogenated
to 0.4 Weight Percent. Approximately Parallel Effects are
Obtained for both Ram Velocities Investigated $(1.26 \times 10^{-4} \text{ms}^{-1}$
$(0.3 \text{ ipm}))$ and $(1.26 \times 10^{-2} \text{ms}^{-1}$ $(3.0 \text{ ipm}))$. Material Hydrogenated
to 0.4 Weight Percent Yields Equivalent Deformation Loads
at Approximately 56°K (100°F) to 83°K (150°F) Lower Temperature

APPENDIX

USE OF THE UPPER BOUND PLASTICITY ANALYSIS OF RING COMPRESSION
TEST DATA TO DETERMINE THE TRUE STRESS-TRUE STRAIN RELATION OF
MATERIALS AT LARGE STRAINS

The first scientific recognition that variations of metal flow
during compression of rings were influenced by interfacial friction
restraints was made by Kudo (Reference 17). This is shown in Figure A-1.
An extensive experimental calibration of this phenomena was performed
initially by Male and Cockcroft (Reference 18) and a detailed material
calibration from the metalworking viewpoint was made by Avitzur (Reference 19).
Saul, Male and DePierre (Reference 20) showed that the mathematical
treatment by Avitzur formed the basis for obtaining the true stress-true
strain relation of materials at conditions of large strain (Reference 20).
Later modifications of the initial mathematical treatment were made by
Avitzur (Reference 21) to account for bulging and non-parallel flow and
then by DePierre and Gurney (Reference 22) to accommodate varying inter-
face friction conditions.

The use of the ring compression test to determine the true stress-
true strain relation of metals is based on a mathematical analysis of the
metal flow during compression. The actual manner in which metal flows under
applied constraints is such that minimum energy is consumed. This natural
law is the basis of the mathematical theorem of plasticity formulated by
Prager and Hodge (Reference 23) which has become known as the Upper Bound
Theorem. The equation form of this theorem is given in Equation A-1.

$$J^* = \frac{2}{\sqrt{3}} \, \sigma_o \int_V \sqrt{1/2 \, \dot{\epsilon}_{ij} \, \dot{\epsilon}_{ij}} \; dV + \int_s \frac{m \, \sigma_o}{\sqrt{3}} \, \Delta V ds \qquad \text{(A-1)}$$

where

J^* is the rate of total energy utilized during the deformation

σ_0 is the flow stress of the material

$\overline{\dot{\varepsilon}}_{ij}$ is the mean effective strain rate

V   is the volume of material undergoing deformation

m   is the interface friction factor (ratio of lubricant shear stress to material shear stress)

v   is the interface velocity

s   is the interface surface area

The use of the upper bound theorem is based on the selection of a deformation velocity field from which a strain rate field $\dot{\varepsilon}_{ij}$, can be derived which satisfies incompressibility conditions throughout the deforming body. The original velocity field derived by Avitzur (Reference 19) is given in cylindrical coordinates in Equations A-2a, A-2b, and A-2c.

$$\dot{U}_\theta = 0 \qquad\qquad\qquad (A\text{-}2a)$$

$$\dot{U}_y = \frac{y}{T}\left(\dot{U}\right) \qquad\qquad\qquad (A\text{-}2b)$$

$$\dot{U}_R = -\frac{1}{2}\left(\frac{\dot{U}}{T}\right)\left(R\right)\left(1 - \frac{R_n^2}{R^2}\right) \qquad\qquad (A\text{-}2c)$$

where

$\dot{U}$ is the cross-head or compression velocity

T   is the thickness of the ring specimen

R_n is the neutral radius

R   is any radial position in the ring specimen, θ, y, and R subscripts represent the circumferential, vertical and radial coordinates

The strain rate field is derived from these velocity equations as shown in Equations A-3a, A-3b, A-3c, and A-3d.

$$\dot{\epsilon}_{RR} = \frac{\partial \dot{U}_R}{\partial R} \qquad (A-3a)$$

$$\dot{\epsilon}_{\theta\theta} = \frac{\dot{U}}{R} + \frac{1}{R} \frac{\partial \dot{U}_\theta}{\partial \theta} \qquad (A-3b)$$

$$\dot{\epsilon}_{yy} = \frac{\partial \dot{U}_y}{\partial y} \qquad (A-3c)$$

$$\dot{\epsilon}_{R\theta} = \dot{\epsilon}_{\theta y} = \dot{\epsilon}_{yR} \qquad (A-3d)$$

The strain rate relation of Equation A-3 was incorporated into Equation A-1 and the deformation energy was minimized with respect to the position of the neutral radius. Results of this minimization allowed two equations to be developed. One equation allowed the interface friction factor to be expressed solely in terms of geometric dimensions of the deformed ring specimen and the second equation allowed the ratio of the deformation pressure to material flow stress to be expressed in terms of the friction factor and geometric dimensions of the deformed ring. The equations are given in Reference 19 and are shown in functional form in Equations A-4a and A-4b:

$$m = f_1 \ (R_o, \ R_i, \ R_n, \ T) \qquad (A-4a)$$
$$\frac{P}{\sigma_o} = f_2 \ (R_o, \ R_i, \ R_n, \ T, \ m) \qquad (A-4b)$$

Analysis of Equation A-4a after two or more increments of deformation allows the determination of the interface friction or m factor to be determined solely as a function of the change in internal diameter with change in thickness. The use of the friction factor together with measured values of deformation load allow the material flow stress to be determined. Using an incremental computer analysis of Equations A-4a and A-4b allows for changes in the material flow stress to be incorporated. This technique incorporates the strain hardening conditions automatically.

Equations A-4a and A-4b were developed on the assumption of constant friction conditions and parallel metal flow. Variations in parallel flow due to bulging were minimized by selecting an initial thin ring geometry with respect to the ring diameter.

In an attempt to account for bulging of the free surfaces of the
ring, a modification of the original velocity field was developed by
Avitzur (Reference 21) which included a bulge parameter, b. This
parameter was allowed to be a function of the geometric dimensions of the
ring and the friction factor. When the bulge parameter was considered,
the velocity field equations became modified as shown in Equations A-5a,
A-5b, and A-5c.

$$\dot{U}_\theta = 0 \tag{A-5a}$$

$$\dot{U}_y = -\frac{\dot{U}}{2} \; \frac{1 - \exp\left(-\frac{by}{T}\right)}{1 - \exp\left(-\frac{b}{2}\right)} \tag{A-5b}$$

$$\dot{U}_r = \frac{b}{4}\left(\frac{\dot{U}}{T}\right)(R)\left(1 - \frac{R_n^2}{R^2}\right)\left[\frac{\exp\left(-\frac{by}{T}\right)}{1 - \exp\left(-\frac{b}{2}\right)}\right] \tag{A-5c}$$

The use of these velocity equations allowed the friction factor and the
deformation pressure to flow stress ratio to be formulated as earlier but
with a modification of the flow to account for bulge. In function form
the equations are expressed in Equations A-6a and A-6b.

$$m = g_1 \; (R_o, \; R_1, \; R_n, \; T, \; b) \tag{A-6a}$$

$$\frac{P}{\sigma_o} = g_2 \; (R_o, \; R_1, \; R_n, \; T, \; b, \; m) \tag{A-6b}$$

These formulations were still based on constant friction conditions
during compression.

The velocity field equation given in Equation A-5c were later used
by DePierre and Gurney (Reference 22) to analyze conditions of deformation
where nonconstant friction conditions occurred. By measuring the internal
and external radii after incremental amounts of deformation, the rate of
change of internal radius with respect to external radius was formulated

and the instantaneous position of the neutral radius was determined from Equation A-5c to obtain the following relationship:

$$\frac{dR_i}{dR_o} = \left[\frac{R_i}{R_o} \right] \left[\frac{1 - \frac{R_n^2}{R_i^2}}{1 - \frac{R_n^2}{R_o^2}} \right] \tag{A-7}$$

The instantaneous value of the neutral radius resultant from Equation A-7 wa then incorporated into the modified Avitzur (Reference 21) analysis with bulge formation as given in Equations A-6a and A-6b together with measured values of deformation load and area to yield the value of material flow stress.

Experimental determination of the material flow stress from the ring compression test consists of compressing a series of rings of identical geometry and metallurgical structure to different incremental levels of deformation but in an otherwise identical manner. Measurements of the final geometry of the rings are shown in Figure A-2. The bulge profile is assumed to be parabolic and an effective internal and external radius is computed. These radii and corresponding deformation loads became input to a computer program in which the neutral radius is computed from Equation A-7 and the solution by the modified Avitzur (Reference 21) analysis is accomplished. Verification of the accuracy of the analysis is made by comparing the results from the ring compression test based on different initial geometries and different friction conditions with results obtained from the Polakowski (Reference 24) re-machined cylinder technique. Results of this comparison are given in Figure A-3 for three different materials tested at room temperature and slow compression rates. The excellent agreement of results provide verification of the analysis.
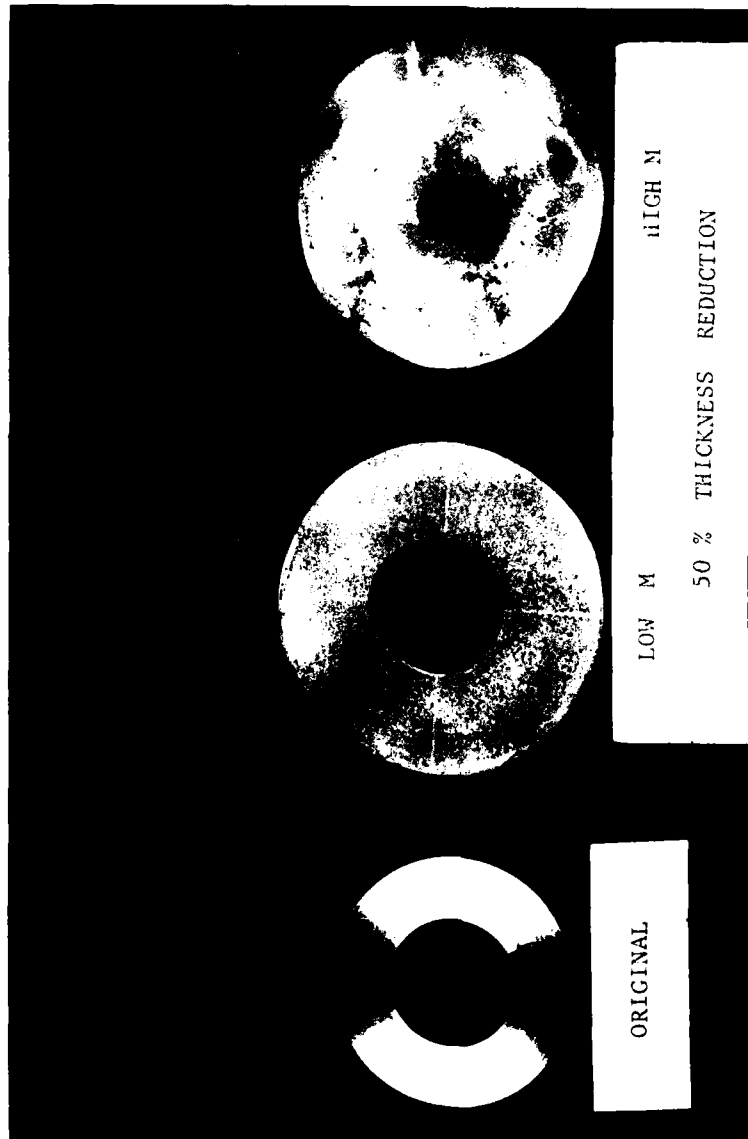
Figure A-1. Effect of Interface Friction on the Change in Internal Diameter of a Ring Shaped Workpiece during Forging. The Factor "m" is the Ratio of the Shear Strength of the Interface Film to the Shear Strength of the Workpiece Material
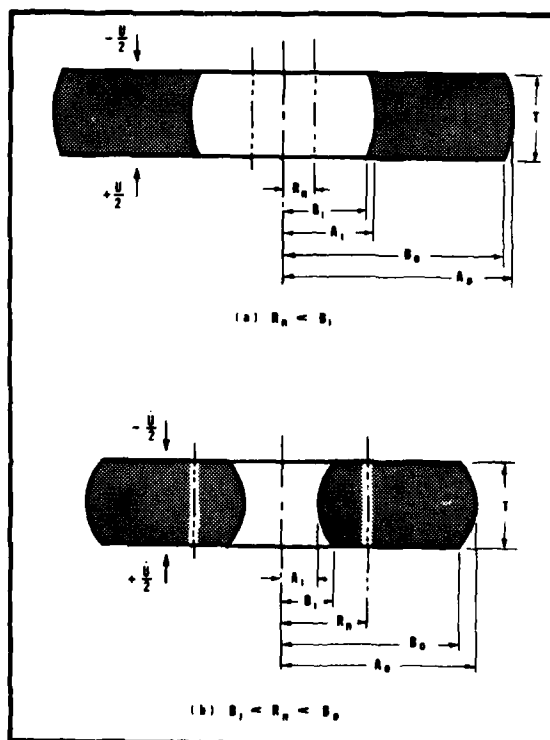
Figure A-2. Schematic Representation
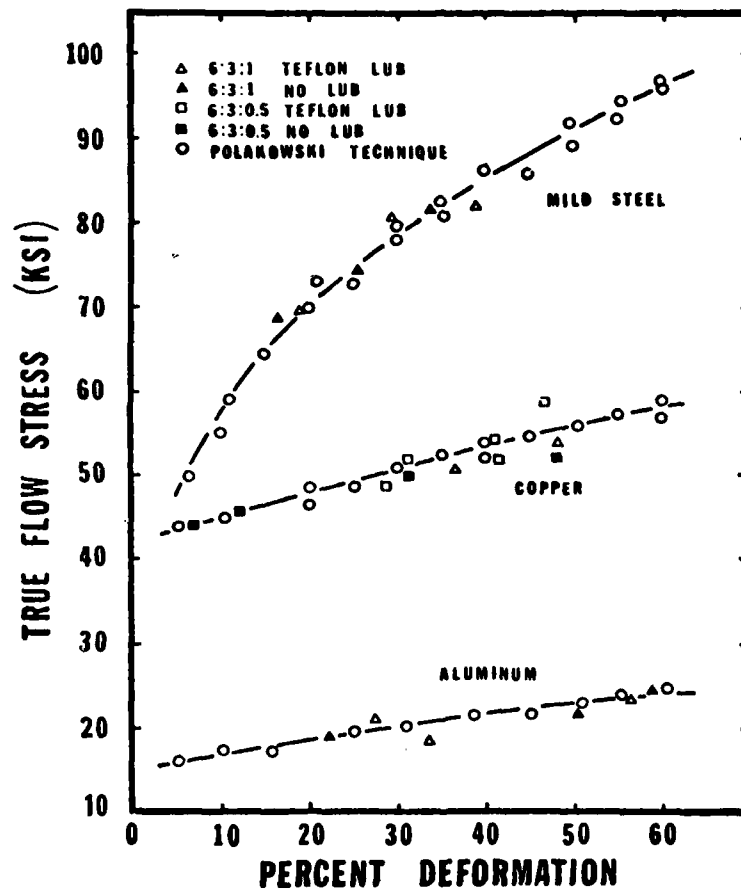of the Ring Geometry
after Forging

Figure A-3. Comparison of the True Stress-True
Strain Results from the Ring
Compression Test with the Polakowski
Re-machined Cylinder Technique

58

REFERENCES

1. M. Hansey, <u>Constitution of Binary Alloys</u>, McGraw-Hill Book Company, Inc., New York, 1958, p. 799.

2. G. A. Lenning, C. M. Craighead and R. I. Jaffee, "Constitution and Mechanical Properties of Titanium-Hydrogen Alloys", TRANS AIME, Journal of Metals, March 1954, p. 367.

3. H. M. Burte, et al., "Hydrogen Embrittlement of Titanium Alloys", Metals Progress, May 1955, p. 115.

4. W. Hohmann, "Powder Metallurgy Production of High Density Titanium Materials", Powder Metallurgy International, <u>6</u>, (2), 1974, p. 66.

5. J. Greenspan, F. J. Rizzitano and E. Scala, "Titanium Powder Metallurgy by DeComposition Sintering of the Hydride", in <u>Titanium Science and Technology</u>, Vol. 1, Ed., R. I. Jaffee and H. M. Burte, Plenum Press, 1973.

6. U. Zwicker, et al., "Process for Improving Workability of Titanium Alloys", U. S. Patent No. 2,892,742, June 1959.

7. B. A. Kolachev, et al., "Effect of Hydrogen on Industrial Plasticity of Ti-9Al", Izvestiya Vysshikh Ucheknykh Zavedeniy Tsvetnaya Metallurgiya, Nr. 4, 1972, pp. 137-142, USAF Foreign Technology Division Translation, FTD-ID(RS)I-1076-76, August 1976.

8. B. A. Kolachev, et al., "Evaluation of the Beneficial Effect of Hydrogen on the Deformability of the Titanium Alloy ST4", Kuzechno-Shtampovochnoye Proizvodstvo, Nr. 1, January 1975, pp. 29-32, USAF Foreign Technology Division Translation, FTD-ID(RS)I-2347-75, November 1975.

9. N. Birla and V. DePierre, "A Test Method for Evaluation of Metal Powders", Air Force Materials Laboratory Technical Report, AFML-TR-75-171, October 1975.

10. F. J. Gurney and A. T. Male, "The Relationship of Microstructure and Mechanical Properties of Extruded Titanium Alloy Bars to the Prior Deformation Processing History", Air Force Materials Laboratory Technical Report AFML-TR-71-28, April 1971.

11. F. J. Gurney and A. T. Male, "Die Temperature Effects in Forging Lubrication", Manufacturing Engineering Transactions, 1975-76, p. 1.

12. Research currently in progress at the Air Force Materials Laboratory, Wright-Patterson Air Force Base, Ohio.

13. Conversations with Wei. Kao of General Dynamics, Inc., Convair, San Diego, Calif., May 1979.

REFERENCES (Continued)

14. A. D. McQuillan, "An Experimental and Thermodynamic Investigation of the Hydrogen-Titanium System", Proceedings of the Royal Society of London, Series A 204, 1951, p. 309.

15. R. J. Wasilewski and G. L. Kehl, "Diffusion of Hydrogen in Titanium", Metallurgica, 49, November 1974, p. 227.

16. W. M. Albrecht and M. W. Mallet, "Hydrogen Solubility and Removal for Titanium and Titanium Alloys", TRANS AIME, 212, April 1958, p. 204.

17. H. Kudo, "Some Analytical and Experimental Studies of Axisymmetric Forging and Extrusion", Int. J. Mechanical Sciences, Part I and Part II, 3, pp. 91-117, 1960-1961.

18. A. T. Male and M. G. Cockcroft, "A Method for the Determination of the Coefficient of Friction of Metals Under Conditions of Bulk Plastic Deformation", J. Inst. Metals, 1964-1965, 93, pp. 38-46.

19. B. Avitzur, Metal Forming: Processes and Analyses, McGraw-Hill, New York, 1968.

20. G. A. Saul, A. T. Male and V. DePierre, "A New Method for the Determination of Material Flow Stress Values Under Metalworking Conditions", Metal Forming Interrelation Between Theory and Practice, Ed., A. L. Hoffmanner, 1971, Plenum Press, New York, pp. 293-306.

21. B. Avitzur, "Bulge in Hollow Disk Forging", Air Force Materials Laboratory Technical Report, TR-69-261, November 1969.

22. V. DePierre and F. J. Gurney, "A Method for Determination of Constant and Varying Friction Factors During Ring Compression Testing", Journal of Lubrication Technology, TRANS ASME, 1974, 96, Series F, (3), p. 482.

23. W. Prager and P. G. Hodge Jr., Theory of Perfectly Plastic Solids, 1951, John Wiley and Sons, Inc., New York, p. 237.

24. N. H. Polakowski, "The Compression Test in Relation to Cold Rolling", J. Iron and Steel Inst., 163, 1949.